*SMAI-JCM*
SMAI Journal of Computational Mathematics

# A multi-scale patch approximation for Poisson problems with a small inhomogeneous inclusion

Saber Amdouni, Mohamed Khaled Gdoura, Arnaud Heibig, Thomas Homolle, Nidhal Mannai, Adrien Petrov & Yves Renard

Volume 11 (2025), p. 139-163.
https://doi.org/10.5802/smai-jcm.121



*The SMAI Journal of Computational Mathematics is a member of the Centre Mersenne for Open Scientific Publishing*
http://www.centre-mersenne.org/
Submissions at https://smai-jcm.centre-mersenne.org/ojs/submission
e-ISSN: 2426-8399

*SMAI Journal of Computational Mathematics*
Vol. 11, 139-163 (2025)

# A multi-scale patch approximation for Poisson problems with a small inhomogeneous inclusion

Saber Amdouni [1]
Mohamed Khaled Gdoura [2]
Arnaud Heibig [3]
Thomas Homolle [4]
Nidhal Mannai [5]
Adrien Petrov [6]
Yves Renard [7]

[1] Laboratory For Mathematical And Numerical Modeling In Engineering Science, LAMSIN, LR99ES20, University of Tunis El Manar, National Engineering School of Tunis, Tunis, Tunisia
*E-mail address*: saber.amdouni@enit.utm.tn
[2] University of Carthage, National Institute of Applied Science and Technology, Centre Urbain Nord BP 676-1080 Tunis Cedex, Tunisia
*E-mail address*: mk.gdoura@insat.ucar.tn
[3] INSA Lyon, ICJ UMR5208, CNRS, Ecole Centrale de Lyon, Universite Claude Bernard Lyon 1, Université Jean Monnet, 69621 Villeurbanne, France
*E-mail address*: arnaud.heibig@insa-lyon.fr
[4] Numerical Modeling and Simulation (FEA) Department of Simulation and Data-Science, Manufacture Française des Pneumatiques Michelin Center of Technologies, Ladoux, Clermont-Ferrand, France
*E-mail address*: thomas.homolle@michelin.com
[5] Laboratory For Mathematical And Numerical Modeling In Engineering Science, LAMSIN, LR99ES20, University of Tunis El Manar, National Engineering School of Tunis, Tunis, Tunisia
*E-mail address*: nidhal.mannai@enit.utm.tn
[6] INSA Lyon, ICJ UMR5208, CNRS, Ecole Centrale de Lyon, Universite Claude Bernard Lyon 1, Université Jean Monnet, 69621 Villeurbanne, France
*E-mail address*: adrien.petrov@insa-lyon.fr
[7] INSA Lyon, ICJ UMR5208, CNRS, Ecole Centrale de Lyon, Universite Claude Bernard Lyon 1, Université Jean Monnet, 69621 Villeurbanne, France
*E-mail address*: yves.renard@insa-lyon.fr.

**Abstract.** The paper deals with the multi-scale approximation of the influence of a small inhomogeneity of arbitrary shape in an elastic medium. A new multi-scale patch method is introduced, whose caracteristic is to deal with a large scale problem without inclusion, a small-scale problem on a patch surrounding the inclusion defining a corrector and an iterative procedure between these two problems. Theoretical results of convergence of the iterations, *a posteriori* error estimate and comparison of the corrector with the asymptotic expansion are provided. The finite element approximation is also addressed together with some numerical tests.

**2020 Mathematics Subject Classification.** 65N12, 65N30, 74Q05, 74Q15.

**Keywords.** Patch method, Asymptotic expansion, finite element method, multi-scale analysis, transmission problem.

The present work is realized as a part of a scientific collaboration with the company "Manufacture Française des Pneumatiques Michelin". The authors are grateful for financial support and rich discussions. It was also financially supported by the University of Tunis El Manar and the "PHC Utique" program of the French Ministry of Foreign Affairs and Ministry of Higher Education, Research and Innovation and the Tunisian Ministry of Higher Education and Scientific Research via the CMCU project number 22G1123.

S. Amdouni is the corresponding author.

https://doi.org/10.5802/smai-jcm.121

## 1. Introduction

An important engineering and mathematical literature is devoted to inclusions embedded in elastic media as for instance in automotive industry to design tires having specific structure stiffnesses. A good understanding of these inclusions influence is crucial to preserve the quality required by the traffic safety and driver comfort as well as to reduce maintenance costs.

We are interested in this work to some small elastic inhomogeneous inclusions in an elastic body. Without adapted treatment, the numerical approximation of this problem requires a mesh refinement near the inclusions which is rather costly from numerical viewpoint, especially when the inclusion is small compared to the domain of interest. The homogenization techniques can be used in the particular case where the inclusions are arranged within a periodic or nearly periodic network. The reader is referred for instance to [19, 26] for further details. However, these techniques are not convenient when one needs to evaluate the influence of isolated inclusions. These inclusions are often omitted in many applications at least for the smallest ones because of the induced computational cost. The asymptotic analysis could be used to determine isolated inclusions influence, see for instance [5, 7, 11, 12, 17, 20, 31, 33] and the references therein.

One of the motivations behind the design of the proposed method is, similarly to the asymptotic study presented in [4], to start from the problem without inclusion and write successive correctors on the solution. This comes from a practical concern in numerical modeling of a complex structure, for instance the whole simulation of a tire, a concern of our industrial partner. Clearly, the addition of a number of meshes adapted to small inclusions to take account of their influence is very penalizing for the complete calculation of the structure. Thus, the primary objective of our method is to keep a complete calculation of the structure with a mesh that does not account for the inclusions and to calculate the influence of the inclusions by a separate local calculation on each inclusion. The remainder of this paper presents the case of a single inclusion, but can easily be generalized to any number of inclusions, provided they remain isolated.

A second important motivation is to produce a method that can be potentially generalized to the case of non-linear constitutive laws, typically hyper-elasticity. It is not the aim of the present paper to present the method in a non-linear framework, but to establish the method in a theoretical framework which is made possible by the linear character of the chosen problem and the study carried out in [4]. Clearly, for the chosen linear transmission problem, other techniques can be also considered, such as the use of boundary integrals (see [1]), the construction of an elastic moment tensor accounting for the effect of the inclusions as in [7], the use of matched asymptotic expansion as in [2, 6], or inverted finite element techniques [9] to derive an enrichment basis for the solution as in [21]. These methods do not generalize well to nonlinear constitutive laws, so we propose a method based on a technique close to domain decomposition techniques.

Consequently, this paper focuses on an approximation of the influence of a small inhomogeneity in an elastic medium by the construction of a patch type method, computing successive approximations of the deformation, starting from the deformation without the inclusion. Unlike the analytical approaches derived from Eshelby's seminal work [15] and various extensions analyzed later on in [3, 16, 23, 24, 25, 29, 32], the considered inclusion is of arbitrary geometry and elastic property. The proposed method is close to the Schwarz type domain decomposition method with total overlap (see [14] for instance) as well as to the patch methods described in [18, 28, 30], except the important difference that the micro and large scale problems do not take into account the same physics. It is also close to the structural zoom methods [10, 13] with the main difference of starting from the solution without inclusion and iterating on correctors to this solution. This last characteristic has the advantage of being less intrusive for an existing finite element code (the large scale computation is performed on the whole geometry without taking into account the inclusion) and it allows the link with the asymptotic analysis developed in [4] and enable us to guarantee some approximation orders.

The paper is organized as follows. A geometrical setting is presented and the solvability is recalled in Section 2. Our *patch method* is introduced in Section 3. This method involves incorporating an intermediate polygonal domain, the so-called influence domain or Patch domain, which contains the inclusion. Hence a corrector is evaluated on the patch domain by using a mesh refinement and added to the solution without inclusion evaluated on the whole domain by using a coarse mesh. This procedure can be iterated to improve the approximation accuracy. Some convergence results of the iterations to the solution of the transmission problem are given. Then, Section 4 makes the link between our patch method and the asymptotic analysis in [4]. In the particular case of Dirichlet condition on the boundary of the domain, it allows us to state an order of convergence with respect to the inclusion and patch sizes for the corrector on the first iteration. Finally, the numerical patch method is introduced in Section 5 with a two-scale finite element approximation and some numerical tests on a simple geometry and a circular inclusion that are compared to the theoretical results of Sections 3 and 4.

## 2. Mathematical formulation of the transmission problem

Let $\Omega$ be a bounded Lipschitz domain in $\mathbb{R}^2$ with a Lipschitz-continuous external boundary $\Gamma = \partial\Omega$. Let $\Omega_f^1$ be a bounded connected domain of characteristic size 2 representing the geometry of the inclusion, and $\Omega_f = \varepsilon\Omega_f^1$ the domain of characteristic size $2\varepsilon$ representing the inclusion, satisfying $\Omega_f \subset \Omega$. Let $\Gamma^\varepsilon = \partial\Omega_f$ be the curve separating the two domains and $\Omega_m \overset{\text{def}}{=} \Omega\backslash\overline{\Omega}_f$ the rest of the domain. The inclusion is assumed to be small enough compared to the characteristic size $R$ of the domain $\Omega$. We assume also that the boundary $\Gamma$ is split into two disjoint sets $\Gamma_{\mathrm{D}}$ and $\Gamma_{\mathrm{N}}$ where Dirichlet and Neumann boundary conditions are considered, respectively. Finally, we denote by $\Lambda$ a *patch domain* supposed to be included in $\Omega$ and containing $\Omega_f$ (for $\varepsilon$ of interest) and by $\partial\Lambda$ its boundary (see Figure 2.1).

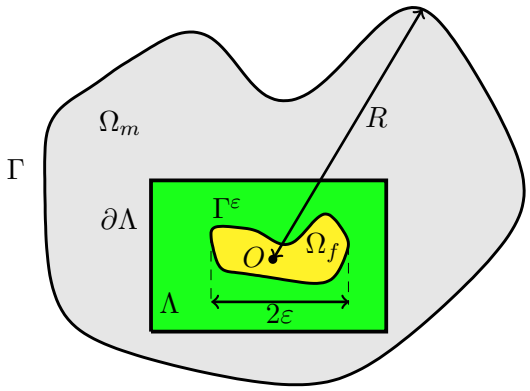


Figure 2.1. A small inclusion in an elastic medium

We focus in this work on a two-dimensional multi-scale problem with discontinuous coefficient $\alpha$ across $\Gamma^\varepsilon$. Let $u : \Omega \to \mathbb{R}^2$, be the displacement of the body $\Omega$ and $h$ be the prescribed Neumann

boundary condition on $\Gamma_{\mathrm{N}}$. The mathematical problem is formulated as follows

$$-\alpha_f \Delta u_f = f \quad \text{in} \quad \Omega_f, \tag{2.1a}$$
$$-\alpha_m \Delta u_m = f \quad \text{in} \quad \Omega_m, \tag{2.1b}$$
$$u_f = u_m \quad \text{on} \quad \Gamma^{\varepsilon}, \tag{2.1c}$$
$$\alpha_f \frac{\partial u_f}{\partial n} = \alpha_m \frac{\partial u_m}{\partial n} \quad \text{on} \quad \Gamma^{\varepsilon}, \tag{2.1d}$$
$$u = 0 \quad \text{on} \quad \Gamma_{\mathrm{D}}, \tag{2.1e}$$
$$\frac{\partial u}{\partial n} = h \quad \text{on} \quad \Gamma_{\mathrm{N}}, \tag{2.1f}$$

where $\frac{\partial}{\partial n}$ denotes the normal derivative, $\alpha_f > 0$ and $\alpha_m > 0$ are the constant shear coefficients in the inclusion and in the matrix, respectively, while $u_f$ and $u_m$ are the restriction of $u$ to $\Omega_f$ and $\Omega_m$, respectively. A perfect transmission conditions of $u$ and its normal derivative is assumed. We denote by $u^0$ the solution to the problem without any inclusion which reads:

$$-\alpha_m \Delta u^0 = f \quad \text{in} \quad \Omega, \tag{2.2a}$$
$$u^0 = 0 \quad \text{on} \quad \Gamma_{\mathrm{D}}, \tag{2.2b}$$
$$\frac{\partial u^0}{\partial n} = h \quad \text{on} \quad \Gamma_{\mathrm{N}}. \tag{2.2c}$$

We describe the weak formulation associated to problems (2.1) and (2.2). To this aim, we introduce the following vector space:

$$\mathcal{V}_0 \stackrel{\text{def}}{=} \{v \in \mathrm{H}^1(\Omega) : \ v_{|\Gamma_{\mathrm{D}}} = 0\}. \tag{2.3}$$

We state the problem (2.1) in a variational form as

$$\begin{cases} \text{find } u \in \mathcal{V}_0 \text{ such that for all } v \in \mathcal{V}_0, \\ \displaystyle\int_{\Omega_m} \alpha_m \nabla u \cdot \nabla v \,\mathrm{d}x + \int_{\Omega_f} \alpha_f \nabla u \cdot \nabla v \,\mathrm{d}x = \int_{\Omega} f v \,\mathrm{d}x + \int_{\Gamma_{\mathrm{N}}} h v \,\mathrm{d}S, \end{cases} \tag{2.4}$$

while the variational form associated to problem (2.2) is given by

$$\begin{cases} \text{find } u^0 \in \mathcal{V}_0 \text{ such that for all } v \in \mathcal{V}_0, \\ \displaystyle\int_{\Omega} \alpha_m \nabla u^0 \cdot \nabla v \,\mathrm{d}x = \int_{\Omega} f v \,\mathrm{d}x + \int_{\Gamma_{\mathrm{N}}} h v \,\mathrm{d}S. \end{cases} \tag{2.5}$$

We assume that $h \in \mathrm{L}^2(\Gamma_{\mathrm{N}})$ and $f \in \mathrm{L}^2(\Omega)$. The existence and uniqueness results to problems (2.4) and (2.5) follow from Lax–Milgram's theorem.

## 3. The proposed patch method

The aim of this section is to introduce our proposed patch method in the continuous framework and to investigate some basic properties: convergence of the iterations and an *a posteriori* error estimate result that allows to estimate if the convergence is reached or not.

Recall that the starting point of our method is $u^0$, the solution which does not take into account the inclusion and is defined on the whole domain $\Omega$. Then, we define a first corrector on the patch $\Lambda$, denoted $w^0$, in such a way for $u^0 + w^0$ to be a better approximation of the solution to the transmission problem. As far as finite element approximation is concerned, the idea is that the mesh used to approximate $u^0$ does not take the geometry of the inclusion into account, and that a more refined mesh should be used to compute the corrector that account for the inclusion. However, in the continuous framework of this section, it will not be discussed and treated in Section 5.1. From this first correction,

the idea is then to propose successive iterations that converge towards the solution of the original transmission problem, by defining successive $u^i$ and $w^i$, $i \in \mathbb{N}$, always with $u^i$ defined on $\Omega$ and $w^i$ a corrector defined on the patch $\Lambda$.

It should be noted that the major difference between our method and domain decomposition methods such as [14] or structural zoom methods such as [10] is that the physics are different on the two scales: the inclusion do not appear directly in the macro problem and is only taken into account on the micro problem on the patch $\Lambda$.

Let us now propose some notations that will be usefull in the following. Let $\langle u, v\rangle_{\alpha,\Omega} \stackrel{\text{def}}{=} \int_\Omega \alpha \nabla u \cdot \nabla v \, \mathrm{d}x$ be the scalar product and $\|u\|^2_{\alpha,\Omega} \stackrel{\text{def}}{=} \int_\Omega \alpha |\nabla u|^2 \, \mathrm{d}x$ the associated norm for all $(u, v) \in \mathrm{H}^1(\Omega) \times \mathrm{H}^1(\Omega)$, where

$$\alpha \stackrel{\text{def}}{=} \begin{cases} \alpha_f & \text{in } \Omega_f, \\ \alpha_m & \text{in } \Omega_m, \end{cases}$$

and let

$$\mathcal{W}_0 \stackrel{\text{def}}{=} \{v \in \mathrm{H}^1(\Omega) : v_{|\Omega\setminus\Lambda} = 0\},$$

be the Hilbert space whose associated scalar product is $\langle \cdot, \cdot \rangle_{\alpha,\Lambda}$. We denote by $\mathrm{Proj}_{\mathcal{W}_0} : \mathrm{H}^1(\Lambda) \to \mathrm{H}^1_0(\Lambda)$ the orthogonal projection onto $\mathcal{W}_0$ relatively to this scalar product. Notice that $\mathcal{W}_0$ is isomorphic to $\mathrm{H}^1_0(\Lambda)$. In the sequel, we denote $C_{\alpha_f,\alpha_m} \stackrel{\text{def}}{=} \sqrt{\frac{|\alpha_m - \alpha_f|}{\alpha_f}}$.

### 3.1. **The multi-scale patch method iteration**

For the sake of simplicity in defining the iterations, we consider the terms $w^{-1} = u^{-1} = 0$. Then, begining by the macroscopic problem, for any given $w^{n-1} \in \mathcal{W}_0$ and $u^{n-1} \in \mathcal{V}_0$, $n \geq 0$, we denote $u^n$ the solution to the following problem on the whole domain $\Omega$:

$$\begin{cases} \text{find } u^n \in \mathcal{V}_0 \text{ such that for all } v \in \mathcal{V}_0, \\ \displaystyle\int_\Omega \alpha_m \nabla u^n \cdot \nabla v \, \mathrm{d}x = \int_\Omega f v \, \mathrm{d}x + \int_{\Gamma_N} h v \, \mathrm{d}S \\ \displaystyle -\int_{\Omega_f} (\alpha_f - \alpha_m) \nabla u^{n-1} \cdot \nabla v \, \mathrm{d}x - \int_\Lambda \alpha \nabla w^{n-1} \cdot \nabla v \, \mathrm{d}x, \end{cases} \tag{3.1}$$

Then, the corrector $w^n$ will be the solution to the following microscopic problem defined on the patch $\Lambda$:

$$\begin{cases} \text{find } w^n \in \mathcal{W}_0 \text{ such that for all } v \in \mathcal{W}_0, \\ \displaystyle\int_\Lambda \alpha \nabla w^n \cdot \nabla v \, \mathrm{d}x = \int_\Lambda f v \, \mathrm{d}x - \int_\Lambda \alpha \nabla u^n \cdot \nabla v \, \mathrm{d}x. \end{cases} \tag{3.2}$$

It can be noted that, since $w^{-1} = u^{-1} = 0$, the solution $u^0$ to (3.1) for $n = 0$ is the solution to the problem without inclusion (2.5). Note also that even for $n > 0$, the terms on $\Omega_f$ in (3.1) are only some source terms. The approximation of Problem (2.4) will be obtained by successive iteration of the two sub-problems (3.1) and (3.2)

### 3.2. **Convergence of the iterations**

We establish below that $u^n + w^n$ converges toward the solution $u$ to problem (2.4) under some conditions on the parameters $\alpha_f$ and $\alpha_m$, or alternatively on the smallness of the inclusion size $\varepsilon$. To this aim, let us introduce the following differences between the solution and the successive approximations:

$$a^n \stackrel{\text{def}}{=} u - (u^n + w^{n-1}) \quad \text{and} \quad b^n \stackrel{\text{def}}{=} u - (u^n + w^n) \tag{3.3}$$

for all $n \in \mathbb{N}$. Observe that $a^n$ and $b^n$ belong to $\mathcal{V}_0$.

Firstly we prove that $\|b^n\|_{\alpha,\Omega} \leq \|a^n\|_{\alpha,\Omega}$ and secondly we discuss the conditions under which $\|a^n\|_{\alpha,\Omega} \leq K \|b^{n-1}\|_{\alpha,\Omega}$ with $K < 1$ in order to ensure that $\|b^n\|_{\alpha,\Omega}$ decreases to zero and that the iterations converge toward the expected solution.

**Lemma 3.1.** *Assume that $u$, $u^n$ and $w^n$ be the solutions to problems* (2.4), (3.1) *and* (3.2), *respectively and* (3.3) *holds. Then, we have*

$$\|b^n\|_{\alpha,\Omega} \leq \|a^n\|_{\alpha,\Omega} \tag{3.4}$$

*for all $n \in \mathbb{N}$.*

**Proof.** Since $u$ is the solution to problem (2.4), we may deduce that

$$\int_\Lambda \alpha \nabla u \cdot \nabla v \, \mathrm{d}x = \int_\Lambda f v \, \mathrm{d}x \tag{3.5}$$

for all $v \in \mathcal{W}_0$. By subtracting (3.5) from (3.2), we get

$$\int_\Lambda \alpha \nabla w^n \cdot \nabla v \, \mathrm{d}x = \int_\Lambda \alpha \nabla (u - u^n) \cdot \nabla v \, \mathrm{d}x$$

for all $v \in \mathcal{W}_0$. Clearly, we may infer that $w^n = \mathrm{Proj}_{\mathcal{W}_0}(u - u^n)$ and it follows that

$$\|u - (u^n + w^n)\|_{\alpha,\Lambda} \leq \left\|u - (u^n + w^{n-1})\right\|_{\alpha,\Lambda}. \tag{3.6}$$

On the other hand, we have

$$\|u - (u^n + w^n)\|^2_{\alpha,\Omega} = \|u - u^n\|^2_{\alpha,\Omega\setminus\Lambda} + \|u - (u^n + w^n)\|^2_{\alpha,\Lambda}. \tag{3.7}$$

Inserting (3.6) into (3.7), the desired result follows. ∎

Note that subtracting (3.5) from (3.2), we obtain the following identity:

$$\int_\Lambda \alpha \nabla b^n \cdot \nabla v \, \mathrm{d}x = 0 \tag{3.8}$$

with $v \in \mathcal{W}_0$. The next step consists to establish that there exists $K(\varepsilon, \alpha_f, \alpha_l) \in ]0,1[$, depending on $\varepsilon$, $\alpha_f$ and $\alpha_m$ such that

$$\|a^n\|_{\alpha,\Omega} \leq K(\varepsilon, \alpha_f, \alpha_l) \left\|b^{n-1}\right\|_{\alpha,\Omega}. \tag{3.9}$$

We deduce from (2.4) and (3.1) that

$$\int_\Omega \alpha_m \nabla u^n \cdot \nabla v \, \mathrm{d}x = \int_\Omega \alpha_m \nabla u \cdot \nabla v \, \mathrm{d}x - \int_\Lambda \alpha_m \nabla w^{n-1} \cdot \nabla v \, \mathrm{d}x + \int_{\Omega_f} (\alpha_f - \alpha_m) \nabla (u - (u^{n-1} + w^{n-1})) \cdot \nabla v \, \mathrm{d}x$$

for all $v \in \mathcal{V}^0$, which according to notations (3.3) implies that

$$\int_\Omega \alpha_m \nabla a^n \cdot \nabla v \, \mathrm{d}x = -\int_{\Omega_f} (\alpha_f - \alpha_m) \nabla b^{n-1} \cdot \nabla v \, \mathrm{d}x \tag{3.10}$$

for all $v \in \mathcal{V}^0$. Choosing $v = a^n$ in (3.10), we get

$$\int_\Omega \alpha \left|\nabla a^n\right|^2 \mathrm{d}x = \int_{\Omega_f} (\alpha_f - \alpha_m) \left|\nabla a^n\right|^2 \mathrm{d}x - \int_{\Omega_f} (\alpha_f - \alpha_m) \nabla b^{n-1} \cdot \nabla a^n \, \mathrm{d}x.$$

According to Cauchy–Schwarz's inequality, we find

$$\|a^n\|^2_{\alpha_m,\Omega_m} + \frac{\alpha_m}{\alpha_f} \|a^n\|^2_{\alpha_f,\Omega_f} = -\frac{\alpha_f - \alpha_m}{\alpha_f} \int_{\Omega_f} \alpha_f \nabla b^{n-1} \cdot \nabla a^n \, \mathrm{d}x \leq C^2_{\alpha_f,\alpha_m} \|a^n\|_{\alpha_f,\Omega_f} \left\|b^{n-1}\right\|_{\alpha_f,\Omega_f}. \tag{3.11}$$

On the one hand, using Young's inequality, we infer from (3.11) that for all $\gamma > 0$ we have

$$\|a^n\|^2_{\alpha_m,\Omega_m} + \frac{\alpha_m}{\alpha_f}\|a^n\|^2_{\alpha_f,\Omega_f} \leq C^2_{\alpha_f,\alpha_m}\Big(\gamma\|a^n\|^2_{\alpha_f,\Omega_f} + \frac{1}{4\gamma}\left\|b^{n-1}\right\|^2_{\alpha_f,\Omega_f}\Big).$$

Taking $\frac{\alpha_m}{\alpha_f} \geq 1$ and $\gamma = 1$, we obtain

$$\|a^n\|^2_{\alpha,\Omega} \leq \frac{1}{4}\Big(\frac{\alpha_m}{\alpha_f} - 1\Big)\left\|b^{n-1}\right\|^2_{\alpha_f,\Omega_f}. \tag{3.12}$$

On the other hand, (3.11) implies that

$$\min\Big(1, \frac{\alpha_m}{\alpha_f}\Big)\|a^n\|_{\alpha,\Omega} \leq C^2_{\alpha_f,\alpha_m}\left\|b^{n-1}\right\|_{\alpha_f,\Omega_f}. \tag{3.13}$$

Hence, defining $\widetilde{C} > 0$ as

$$\widetilde{C} \stackrel{\text{def}}{=} \begin{cases} \dfrac{1}{4}\Big(\dfrac{\alpha_m}{\alpha_f} - 1\Big) & \text{if } \dfrac{\alpha_m}{\alpha_f} \geq 1, \\ \dfrac{C^2_{\alpha_f,\alpha_m}}{\min\Big(1, \frac{\alpha_m}{\alpha_f}\Big)} & \text{elsewhere,} \end{cases} \tag{3.14}$$

we may deduce from (3.12) and (3.13) that for $\frac{1}{2}\alpha_f < \alpha_m < 5\alpha_f$, $\|b^n\|_{\alpha,\Omega} \leq \widetilde{C}\left\|b^{n-1}\right\|_{\alpha,\Omega}$ with $\widetilde{C} < 1$. Consequently, $b^n$ converges to 0 in $\mathrm{H}^1(\Omega)$ under this condition. However, this result can be improved as we will see later on. To this aim, we define the two following auxiliary problems:

$$\begin{cases} \text{find } \zeta \in \mathrm{H}^1(\Lambda) \text{ with } \zeta = q \text{ on } \partial\Lambda \text{ such that for all } z \in \mathcal{W}_0, \\ \langle\zeta, z\rangle_{\alpha_m,\Lambda} \stackrel{\text{def}}{=} \displaystyle\int_\Lambda \alpha_m \nabla\zeta\cdot\nabla z\,\mathrm{d}x = 0, \end{cases} \tag{3.15}$$

and

$$\begin{cases} \text{find } \eta \in \mathrm{H}^1(\Lambda) \text{ with } \eta = q \text{ on } \partial\Lambda \text{ such that for all } z \in \mathcal{W}_0, \\ \langle\eta, z\rangle_{\alpha,\Lambda} \stackrel{\text{def}}{=} \displaystyle\int_\Lambda \alpha\nabla\eta\cdot\nabla z\,\mathrm{d}x = 0. \end{cases} \tag{3.16}$$

The existence and uniqueness results to problems (3.15) and (3.16) follow from Lax–Milgram's theorem, the verification is left to the reader. Under appropriate regularity assumptions on boundary conditions, we establish below that $\|\zeta\|_{\alpha_f,\Omega_f}$ and $\|\eta\|_{\alpha_f,\Omega_f}$ are of order $\mathcal{O}(\varepsilon)$. In the sequel, we will use the following notations: $\mathcal{X} \stackrel{\text{def}}{=} \mathrm{H}^{1/2}(\partial\Lambda)$ and $\mathcal{X}' \stackrel{\text{def}}{=} \mathrm{H}^{-1/2}(\partial\Lambda)$. We will also denote $\varepsilon \stackrel{\text{def}}{=} \sup[(x-x')^2 + (y-y')^2]^{1/2}$, the sup being taken on $(x,y),(x',y') \in \Omega_f \times \Omega_f$ and $\mathrm{dist}(0,\partial\Lambda)$ the distance between 0 and $\partial\Lambda$.

**Lemma 3.2.** *Assume that $q \in \mathcal{X}$ and $\zeta$ be the solution to problem* (3.15). *Then*

$$\|\zeta\|_{\alpha_f,\Omega_f} \leq \frac{4\sqrt{2\alpha_f}}{\mathrm{dist}(0,\partial\Lambda)}\varepsilon\|q\|_{\mathcal{X}}. \tag{3.17}$$

**Proof.** Let $0 < \varepsilon < \varepsilon_0$ with $\varepsilon_0$ small enough. We assume that $\varepsilon_0$ is chosen so small that $\Omega_f \subset C_{\varrho/2} \subset C_\varrho \subset \Lambda$ for $\frac{1}{2}\mathrm{dist}(0,\partial\Lambda) \leq \varrho < \mathrm{dist}(0,\partial\Lambda)$. Here, $C_\varrho$ denotes a disk with radius $\varrho > 0$ centered at the origin. For any $(x,y) \in C_{\varrho/2}$, we set $z \stackrel{\text{def}}{=} x + iy$. Using the Poisson kernel, we get $\zeta(x,y) = \mathcal{R}f(z)$ with $f(z) = \frac{1}{2\pi}\int_{-\pi}^{\pi}\frac{\varrho\mathrm{e}^{i\theta}+z}{\varrho\mathrm{e}^{i\theta}-z}\zeta(\varrho\cos(\theta),\varrho\sin(\theta))\,\mathrm{d}\theta$. Since $|z| \leq \varrho/2$, we have

$$|f'(z)| \leq \frac{1}{\pi}\int_{-\pi}^{\pi}\Big|\frac{\varrho\mathrm{e}^{i\theta}}{(\varrho\mathrm{e}^{i\theta}-z)^2}\Big|\,|\zeta(\varrho\cos(\theta),\varrho\sin(\theta))|\,\mathrm{d}\theta \leq \frac{4\sqrt{2}}{\varrho\sqrt{\pi}}\|\zeta\|_{\mathrm{L}^2(\partial C_\varrho)}.$$

The euclidian norm $|\nabla\zeta(x,y)|$ satisfies the same inequality, which by integration over $\Omega_f$ gives

$$\|\zeta\|^2_{\alpha_f,\Omega_f} \leq \frac{32\alpha_f}{\pi\varrho^2}\,|\Omega_f|\,\|\zeta\|^2_{\mathrm{L}^2(\partial C_\varrho)} \leq \frac{32\alpha_f\varepsilon^2}{\varrho^2}\,\|\zeta\|^2_{\mathrm{H}^1(\Lambda)} \leq \frac{32\alpha_f\varepsilon^2}{\varrho^2}\,\|q\|^2_{\mathcal{X}}$$

for $0<\varepsilon<\varepsilon_0$. Replacing $\varrho$ by $\mathrm{dist}(0,\partial\Lambda)$, we get (3.17). ∎

**Lemma 3.3.** *Assume that $q\in\mathcal{X}$ and $\eta$ be the solution to problem* (3.16)*. Then, defining $\overline{K}=\max\{\alpha_f,\alpha_m\}\,\frac{4(1+C^2_{\alpha_f,\alpha_m})\sqrt{2\alpha_f}}{\mathrm{dist}(0,\partial\Lambda)}$, one has*

$$\|\eta\|_{\alpha_f,\Omega_f} \leq \overline{K}\,\varepsilon\,\|\eta\|_{\alpha,\Lambda}\,.$$

**Proof.** Let us define $\nu \overset{\text{def}}{=} \zeta-\eta$ where $\zeta$ and $\eta$ are the solution to problems (3.15) and (3.16), respectively. Hence it comes that

$$\int_\Lambda \alpha\nabla\nu\cdot\nabla z\,\mathrm{d}x = \int_{\Omega_f}(\alpha_m-\alpha_f)\nabla\zeta\cdot\nabla z\,\mathrm{d}x,$$

for all $z\in\mathcal{W}_0$. Since $\nu\in\mathcal{W}_0$, we get

$$\|\nu\|_{\alpha,\Lambda} \leq C^2_{\alpha_f,\alpha_m}\,\|\zeta\|_{\alpha_f,\Omega_f}\,. \tag{3.18}$$

It follows by using the triangular inequality and (3.18) that

$$\|\eta\|_{\alpha_f,\Omega_f} \leq \left(1+C^2_{\alpha_f,\alpha_m}\right)\|\zeta\|_{\alpha_f,\Omega_f}\,.$$

Hence, Lemma 3.2 and trace inequality lead to

$$\|\eta\|_{\alpha_f,\Omega_f} \leq \overline{C}\varepsilon\,\|q\|_{\mathcal{X}} \leq \max\{\alpha_f,\alpha_m\}\,\overline{C}\varepsilon\,\|\eta\|_{\alpha,\Lambda}\,,$$

with $\overline{C}=\frac{4(1+C^2_{\alpha_f,\alpha_m})\sqrt{2\alpha_f}}{\mathrm{dist}(0,\partial\Lambda)}$, which completes the proof. ∎

Finally, we prove below that there exists a positive constant $K<1$ such that

$$\|b^n\|_{\alpha,\Omega} \leq K\left\|b^{n-1}\right\|_{\alpha,\Omega} \tag{3.19}$$

for any $n\in\mathbb{N}$, provided $\varepsilon>0$ is small enough.

**Proposition 3.4.** *Assume that the assumptions of Lemma 3.3 hold. Then, for $\varepsilon$ small enough and any $n\in\mathbb{N}$,* (3.19) *holds true with $K\overset{\text{def}}{=}\overline{K}\,\widetilde{C}\,\varepsilon$ and $\widetilde{C}$ defined by 3.14.*

**Proof.** According to Lemma 3.1, we have $\|b^n\|_{\alpha,\Omega}\leq\|a^n\|_{\alpha,\Omega}$. Since $\|a^n\|_{\alpha,\Omega}\leq\widetilde{C}\left\|b^{n-1}\right\|_{\alpha_f,\Omega_f}$ (see (3.13)), we obtain

$$\|b^n\|_{\alpha,\Omega} \leq \widetilde{C}\left\|b^{n-1}\right\|_{\alpha_f,\Omega_f}\,. \tag{3.20}$$

Appealing to (3.8) and Lemma 3.3, with $\eta=b^{n-1}$, we have

$$\left\|b^{n-1}\right\|_{\alpha_f,\Omega_f} \leq \overline{K}\,\widetilde{C}\,\varepsilon\left\|b^{n-1}\right\|_{\alpha,\Lambda}\,. \tag{3.21}$$

Finally, (3.20) and (3.21) lead to (3.19). ∎

### 3.3. **A posteriori error estimate**

Let us introduce a result that allows to estimate the error norm $\|b^k\|_{\alpha,\Omega}$ with respect to a norm of the correctors on the boundary of the patch. This result is of practical interest to compute an estimation of the error in a numerical procedure.

**Lemma 3.5.** *Still considering* $b^k \stackrel{\text{def}}{=} u - (u^k + w^k)$*, for all* $k \geq 1$*, we have*

$$\|b^k\|_{\alpha,\Omega} \leq C\Big\|\frac{\partial w^{k-1}}{\partial n} - \frac{\partial w^k}{\partial n}\Big\|_{\mathcal{X}'}.$$

**Proof.** If $g$ is a function defined on $\Omega$, we denote by $g_1$ and $g_2$ the restrictions to $\Omega\backslash\overline{\Lambda}$ and $\Lambda\backslash\overline{\Omega}_f$, respectively. Let $n$ be the unit outward normal to the boundary of $\Lambda$.
From (3.8), we have $\Delta b^k = 0$ on $\Lambda$. Hence, by using Green's formula, we get

$$\int_\Lambda \alpha\nabla b^k \cdot \nabla v\,\mathrm{d}x = \Big\langle \alpha_m \frac{\partial}{\partial n}(u_2 - (u_2^k + w_2^k)), v\Big\rangle_{\mathcal{X}',\mathcal{X}} \tag{3.22}$$

for all $v \in \mathrm{H}^1(\Omega)$. Let us define $\widetilde{\mathcal{V}}_0 \stackrel{\text{def}}{=} \{v \in \mathcal{V}_0, v_{|\Lambda} = 0\}$. Observe that $b^k$ is a solution to the following problem:

$$\begin{cases} \displaystyle\int_{\Omega\backslash\Lambda} \alpha\nabla b^k \cdot \nabla v\,\mathrm{d}x = 0 \text{ for all } v \in \widetilde{\mathcal{V}}_0, \\ \displaystyle b^k = 0 \text{ on } \Gamma_{\mathrm{D}}, \quad \frac{\partial b^k}{\partial n} = 0 \text{ on } \Gamma_{\mathrm{N}}. \end{cases} \tag{3.23}$$

It follows that $\Delta b^k_{|\Omega\backslash\Lambda} = 0$ and therefore by Green's formula leads to

$$\int_{\Omega\backslash\Lambda} \alpha\nabla b^k \cdot \nabla v\,\mathrm{d}x = -\Big\langle \alpha_m \frac{\partial}{\partial n}(u_1 - u_1^k - w_1^k), v\Big\rangle_{\mathcal{X}',\mathcal{X}} \tag{3.24}$$

for all $v \in \mathcal{V}_0$. Hence, by (3.22) and (3.24), we have

$$\int_\Omega \alpha\nabla b^k \cdot \nabla v\,\mathrm{d}x = \Big\langle \alpha_m \frac{\partial}{\partial n}(u_2 - u_2^k - w_2^k) - \alpha_m \frac{\partial}{\partial n}(u_1 - u_1^k - w_1^k), v\Big\rangle_{\mathcal{X}',\mathcal{X}} \tag{3.25}$$

for all $v \in \mathcal{V}_0$. Next, notice that $(u - u^k - w^{k-1}) \in \mathrm{H}^1(\Omega)$ satisfies

$$\int_{\Omega_m} \alpha_m \nabla(u - u^k - w^{k-1}) \cdot \nabla v\,\mathrm{d}x = 0$$

for all $v \in \mathrm{H}^1_0(\Omega_m)$, due to (2.4), (3.1) and $w^{k-1} = 0$ on $\Omega\backslash\Lambda$. Hence we have $\Delta\big((u - u^k - w^{k-1})_{|\Omega_m}\big) = 0$ and $\Delta\big((u - u^k - w^{k-1})_{|\Omega_m}\big) \in \mathrm{L}^2(\Omega_m)$. Since $\partial\Lambda \subset \Omega_m$, we get the following jump relation:

$$\frac{\partial}{\partial n}(u_2 - u_2^k - w_2^{k-1}) - \frac{\partial}{\partial n}(u_1 - u_1^k - w_1^{k-1}) = 0 \text{ on } \partial\Lambda. \tag{3.26}$$

According to (3.25), (3.26) and $w_1^k = w_1^{k-1} = 0$, we obtain

$$\int_\Omega \alpha\nabla b^k \cdot \nabla v\,\mathrm{d}x = -\Big\langle \alpha_m \frac{\partial}{\partial n}(w_2^{k-1} - w_2^k), v\Big\rangle_{\mathcal{X}',\mathcal{X}} \tag{3.27}$$

for all $v \in \mathcal{V}_0$. Taking $v = b^k$ in (3.27), using Cauchy–Schwarz's and trace inequalities, the desired result follows. ∎

**Remark 3.6.** Note that from a numerical viewpoint, the $X'$-norm is difficult to compute. However, in a numerical context, it would be sufficient to compute a $L^2(\partial\Lambda)$-norm, the result of Lemma 3.5 being still valid with this norm and the two norms being equivalent for a fixed mesh size.

## 4. The patch method and asymptotic analysis approaches

The aim of this section is to describe the link between the first iteration of our patch method (namely $u^0$ and $w^0$) and the asymptotic analysis given in [4, 22]. This link allows us to provide an error estimate between the result of the first iteration and the solution to the original problem, exhibiting a linear dependency of the error with respect to the patch size and a quadratic dependency with respect to the inclusion size. This study is restricted to the case $\Gamma_{\mathrm{D}} = \partial\Omega$ since the asymptotic analysis has only

been developed in this framework. The main result is given by Lemma 4.3 which provides an estimate of the difference between the corrector of the first iteration of the proposed patch method and the first term of the asymptotic expansion. Then Lemma 4.4 gives an estimate of the normal derivative of the corrector, which also gives an error estimate due to Lemma 3.5 and the fact that $w^{-1} = 0$.

Let us recall that the first order expansion of the problem with the small inclusion can be written

$$u(x) = u^0(x) + \varepsilon W^0\Big(\frac{x}{\varepsilon}\Big) + \mathcal{O}(\varepsilon^2),$$

where $W^0$ is the solution to the following problem

$$\begin{cases} \text{find } W^0 \in \widetilde{\mathcal{V}}^{R^0}_{\log} \text{ such that for all } v \in \widetilde{\mathcal{V}}^{R^0}_{\log}, \\ \displaystyle\int_{\Omega^1_f} (\alpha_f - \alpha_m)\nabla u^{(0)}(0)\cdot\nabla v\,\mathrm{d}x + \int_{\Omega^1_f} \alpha_f \nabla W^0\cdot\nabla v\,\mathrm{d}x + \int_{\Omega^\infty} \alpha_m \nabla W^0\cdot\nabla v\,\mathrm{d}x = 0, \end{cases} \tag{4.1}$$

where $\Omega^1_f$ is $\Omega_f$ for $\varepsilon = 1$, $\Omega^\infty = \mathbb{R}^d \setminus \Omega^1_f$, and for a fixed $R^0 > 1$, the space $\widetilde{\mathcal{V}}^{R^0}_{\log}$ is a closed subspace of

$$\mathcal{V}_{\log} \overset{\text{def}}{=} \{v \in \mathcal{D}'(\mathbb{R}^2) : (1+|x|^2)^{-1/2}(\log(2+|x|^2))^{-1} v \in \mathrm{L}^2(\mathbb{R}^2) \text{ and } \nabla v \in \mathrm{L}^2(\mathbb{R}^2)^2\},$$

defined by

$$\widetilde{\mathcal{V}}^{R^0}_{\log} \overset{\text{def}}{=} \Big\{ v \in \widetilde{\mathcal{V}}_{\log} : \int_{-\pi}^{\pi} v(R^0\cos(\theta), R^0\sin(\theta))\,\mathrm{d}\theta = 0 \Big\},$$

and endowed with the norm

$$\|v\|_{\widetilde{\mathcal{V}}^{R^0}_{\log}} \overset{\text{def}}{=} \big(\|(1+|x|^2)^{-1/2}(\log(2+|x|^2))^{-1} v\|^2_{\mathrm{L}^2(\mathbb{R}^2)} + \|\nabla v\|^2_{\mathrm{L}^2(\mathbb{R}^2)}\big)^{1/2}.$$

For the self consistence of the paper, the estimate on the rest of the first order expansion is recalled below (see for instance [22]). The rest of the section will be dedicated to demonstrate that the difference between the corrector of the patch method $w^0$ and $\varepsilon W^0\big(\frac{\cdot}{\varepsilon}\big)$ is of order $\mathcal{O}\big(\frac{\varepsilon^2}{\mathrm{diam}(\Lambda)}\big)$. We give also the result that $\big\|\frac{\partial w^0}{\partial n}\big\|_{\mathrm{H}^{-1/2}(\partial\Lambda)}$ is of order $\mathcal{O}\big(\frac{\varepsilon^2}{\mathrm{diam}(\Lambda)^{3/2}}\big)$. These results gives also some estimates on the rest $u - (u^0 + w^0)$.

**Lemma 4.1.** *There exists a constant $C > 0$, independent of $\varepsilon$, such that*

$$\Big\| u - u^0 - \varepsilon W^0\Big(\frac{\cdot}{\varepsilon}\Big)\Big\|_{\mathrm{H}^1(\Omega)} \le C\varepsilon^2. \tag{4.2}$$

**Proof.** The corrector $W^0$ satisfies

$$\int_{\Omega_f} (\alpha_f - \alpha_m)\nabla u^{(0)}(0)\cdot\nabla v\,\mathrm{d}x + \int_{\Omega_f} \alpha_f \nabla\Big(\varepsilon W^0\Big(\frac{\cdot}{\varepsilon}\Big)\Big)\cdot\nabla v\,\mathrm{d}x + \int_{\Omega_m} \alpha_m \nabla\Big(\varepsilon W^0\Big(\frac{\cdot}{\varepsilon}\Big)\Big)\cdot\nabla v\,\mathrm{d}x = 0 \tag{4.3}$$

for all $v \in \mathrm{H}^1_0(\Omega)$. On the other hand, by subtracting (2.4) from (2.5), we obtain

$$\int_{\Omega_f} (\alpha_f - \alpha_m)\nabla u^0\cdot\nabla v\,\mathrm{d}x + \int_{\Omega_f} \alpha_f \nabla(u - u^0)\cdot\nabla v\,\mathrm{d}x + \int_{\Omega_m} \alpha_m \nabla(u - u^0)\cdot\nabla v\,\mathrm{d}x = 0. \tag{4.4}$$

Then, it comes by subtracting (4.4) from (4.3) that

$$\begin{aligned} \int_{\Omega_f} (\alpha_f - \alpha_m)(\nabla u^{(0)} - \nabla u^{(0)}(0))\cdot\nabla v\,\mathrm{d}x + \int_{\Omega_f} \alpha_f \nabla\Big(u - u^{(0)} - \varepsilon W^0\Big(\frac{\cdot}{\varepsilon}\Big)\Big)\cdot\nabla v\,\mathrm{d}x \\ + \int_{\Omega_m} \alpha_m \nabla\Big(u - u^{(0)} - \varepsilon W^0\Big(\frac{\cdot}{\varepsilon}\Big)\Big)\cdot\nabla v\,\mathrm{d}x = 0 \end{aligned} \tag{4.5}$$

for all $v \in \mathrm{H}^1_0(\Omega)$.

Let $\bar{\mathcal{L}} : \mathrm{H}^{1/2}(\Gamma) \to \mathrm{H}^1(\Omega)$ be a continuous lifting operator (see for instance [27]). We define $z^\varepsilon \stackrel{\text{def}}{=} \bar{\mathcal{L}}(-\varepsilon W^0(\frac{\cdot}{\varepsilon}))$ and $\xi^\varepsilon \stackrel{\text{def}}{=} u - u^0 - \varepsilon W^0(\frac{\cdot}{\varepsilon}) - z^\varepsilon$. Note that for $v \in \mathrm{H}^1_0(\Omega)$ and by using (4.5), we find

$$\int_{\Omega_f} \alpha_f \nabla\xi^\varepsilon \cdot \nabla v \,\mathrm{d}x + \int_{\Omega_m} \alpha_m \nabla\xi^\varepsilon \cdot \nabla v \,\mathrm{d}x + \int_{\Omega_f} (\alpha_f - \alpha_m)(\nabla u^0(0) - \nabla u^0) \cdot \nabla v \,\mathrm{d}x$$
$$= -\int_{\Omega_f} \alpha_f \nabla z^\varepsilon \cdot \nabla v \,\mathrm{d}x - \int_{\Omega_m} \alpha_m \nabla z^\varepsilon \cdot \nabla v \,\mathrm{d}x. \quad (4.6)$$

Choosing $v = \xi^\varepsilon \in \mathrm{H}^1_0(\Omega)$ in (4.6), we get

$$\alpha_f \|\nabla\xi^\varepsilon\|^2_{\mathrm{L}^2(\Omega_f)} + \alpha_m \|\nabla\xi^\varepsilon\|^2_{\mathrm{L}^2(\Omega_m)} + \int_{\Omega_f} (\alpha_f - \alpha_m)(\nabla u^0(0) - \nabla u^0) \cdot \nabla\xi^\varepsilon \,\mathrm{d}x$$
$$= -\int_{\Omega_f} \alpha_f \nabla z^\varepsilon \cdot \nabla\xi^\varepsilon \,\mathrm{d}x - \int_{\Omega_m} \alpha_m \nabla z^\varepsilon \cdot \nabla\xi^\varepsilon \,\mathrm{d}x,$$

which by using Cauchy–Schwarz's inequality leads to

$$\|\nabla\xi^\varepsilon\|_{\mathrm{L}^2(\Omega)} \le C\Big(\big\|\nabla u^0(0) - \nabla u^0\big\|_{\mathrm{L}^2(\Omega_f)} + \|\nabla z^\varepsilon\|_{\mathrm{L}^2(\Omega)}\Big).$$

According to Poincaré's inequality, we find

$$\|\xi^\varepsilon\|_{\mathrm{H}^1(\Omega)} \le C\Big(\big\|\nabla u^0(0) - \nabla u^0\big\|_{\mathrm{L}^2(\Omega_f)} + \|z^\varepsilon\|_{\mathrm{H}^1(\Omega)}\Big).$$

Notice that $\xi^\varepsilon = u - u^0 - \varepsilon W^0(\frac{\cdot}{\varepsilon}) - z^\varepsilon$ allows to infer that

$$\Big\|u - u^0 - \varepsilon W^0\Big(\frac{\cdot}{\varepsilon}\Big)\Big\|_{\mathrm{H}^1(\Omega)} \le C\Big(\big\|\nabla u^0(0) - \nabla u^0\big\|_{\mathrm{L}^2(\Omega_f)} + \|z^\varepsilon\|_{\mathrm{H}^1(\Omega)}\Big). \quad (4.7)$$

By using the continuity of the lifting operator from $\mathrm{H}^{1/2}(\Gamma)$ to $\mathrm{H}^1(\Omega)$, we get

$$\Big\|u - u^0 - \varepsilon W^0\Big(\frac{\cdot}{\varepsilon}\Big)\Big\|_{\mathrm{H}^1(\Omega)} \le C\Big(\big\|\nabla u^0(0) - \nabla u^0\big\|_{\mathrm{L}^2(\Omega_f)} + \varepsilon\Big\|W^0\Big(\frac{\cdot}{\varepsilon}\Big)\Big\|_{\mathrm{H}^{1/2}(\Gamma)}\Big). \quad (4.8)$$

We evaluate now separately the two terms on the right hand side of (4.8). On the one hand, we observe that

$$\nabla u^0(x) = \nabla u^0(0) + \mathcal{O}(|x|).$$

Consequently, we find

$$\big\|\nabla u^0(x) - \nabla u^0(0)\big\|_{\mathrm{L}^2(\Omega_f)} \le C\,\|x\|_{\mathrm{L}^2(\Omega_f)} \le C\varepsilon^2. \quad (4.9)$$

On the other hand, the last term on the right hand side of (4.8) can be evaluated thanks to an expansion of $W^0$ in polar coordinates. Let $x \stackrel{\text{def}}{=} (r\cos(\theta), r\sin(\theta))$ for all $r \ge \varepsilon R_0$ with $R_0 > 1$. Since $W^0$ is an harmonic function, for all $n \in \mathbb{N}^*$ and $\theta \in [0, 2\pi]$, there exists $(\widetilde{a}_n, \widetilde{b}_n) \in \mathbb{R}^2$ such that

$$W^0\Big(\frac{x}{\varepsilon}\Big) = \sum_{n\ge1} \Big(\frac{\varepsilon R_0}{r}\Big)^n (\widetilde{a}_n \cos(n\theta) + \widetilde{b}_n \sin(n\theta)). \quad (4.10)$$

Let $\Omega_c$ be a subset of $\mathbb{R}^2$ with $\Gamma \subset \mathring{\Omega}_c$, such that there exists $(\varrho_1, \varrho_2) \in \mathbb{R}^2$ with $\varrho_1 < |x| < \varrho_2$, for all $x \in \Omega_c$. Then, the trace inequality leads to

$$\Big\|W^0\Big(\frac{\cdot}{\varepsilon}\Big)\Big\|_{\mathrm{H}^{1/2}(\Gamma)} \le C\|W^0\Big(\frac{\cdot}{\varepsilon}\Big)\Big\|_{\mathrm{H}^1(\Omega_c)}. \quad (4.11)$$

Choosing $\varepsilon > 0$ such that $\varepsilon < \frac{\varrho_1}{R_0}$, we get

$$\Big\|W^0\Big(\frac{\cdot}{\varepsilon}\Big)\Big\|^2_{\mathrm{L}^2(\Omega_c)} \le \frac{2\varepsilon^2 R_0^2 |\Omega_c|}{\varrho_1^2} \sum_{k\ge1} \Big(\frac{\varepsilon R_0}{\varrho_1}\Big)^{2(k-1)} (|\widetilde{a}_k|^2 + |\widetilde{b}_k|^2) \le C\varepsilon^2, \quad (4.12a)$$

$$\Big\|\nabla W^0\Big(\frac{\cdot}{\varepsilon}\Big)\Big\|^2_{\mathrm{L}^2(\Omega_c)} \le \frac{4\varepsilon^2 R_0^2 |\Omega_c|}{\varrho_1^2} \sum_{k\ge1} k^2 \Big(\frac{\varepsilon R_0}{\varrho_1}\Big)^{2(k-1)} (|\widetilde{a}_k|^2 + |\widetilde{b}_k|^2) \le C\varepsilon^2, \quad (4.12b)$$

where $|\Omega_c|$ stands for the usual measure of $\Omega_c$. Introducing (4.12) into (4.11), we get

$$\left\|W^0\left(\frac{\cdot}{\varepsilon}\right)\right\|_{\mathrm{H}^{1/2}(\Gamma)} \leq C\varepsilon. \tag{4.13}$$

Carrying (4.9) and (4.13), we finally obtain (4.2). ∎

In order to make a comparison with respect to the size of the inclusion $\varepsilon$ and the size of the patch, without changing its geometry, we introduce a fixed size patch $\widetilde{\Lambda} \subset \Omega$ (such that $\partial\widetilde{\Lambda} \cap \partial\Omega = \emptyset$). We consider $\Lambda = \frac{\widetilde{\Lambda}}{p}$ with $p > 1$. It is also convenient to introduce the following notation:

$$\begin{array}{rccc} h_p: & \widetilde{\Lambda} & \longrightarrow & \Lambda \\ & u & \longmapsto & u/p. \end{array}$$

In the sequel, we denote by $\mathcal{L} : \mathrm{H}^{1/2}(\partial\widetilde{\Lambda}) \to \mathrm{H}^1(\widetilde{\Lambda})$ the continuous harmonic lifting operator in the fixed configuration. We define $\mathcal{L}_p : \mathcal{X} \to \mathrm{H}^1(\Lambda)$ as the scaled harmonic lifting operator, for all $f_p \in \mathcal{X}$ and $x \in \Lambda$, we get

$$(\mathcal{L}_p(f_p))(x) = (\mathcal{L}f)(px)$$

with $f(z) \overset{\text{def}}{=} f_p(z/p)$ for any $z \in \partial\widetilde{\Lambda}$. Notice that

$$\|\nabla(\mathcal{L}_p f_p)\|^2_{\mathrm{L}^2(\Lambda)} = \|\nabla(\mathcal{L}f)\|^2_{\mathrm{L}^2(\widetilde{\Lambda})}. \tag{4.14}$$

The following estimate between $W^0(\frac{\cdot}{\varepsilon})$ and $\mathrm{Proj}_{\mathcal{W}_0}(W^0(\frac{\cdot}{\varepsilon}))$ is an intermediate result which allow us to get an estimate between $w^0$ and $W^0(\frac{\cdot}{\varepsilon})$.

**Lemma 4.2.** *There exists a constant $C > 0$, independent of $\varepsilon$ and $p$, such that*

$$\left\|W^0\left(\frac{\cdot}{\varepsilon}\right) - \mathrm{Proj}_{\mathcal{W}_0}\left(W^0\left(\frac{\cdot}{\varepsilon}\right)\right)\right\|_{\alpha,\Lambda} \leq Cp\varepsilon. \tag{4.15}$$

**Proof.** Let $W_p \overset{\text{def}}{=} W^0(\frac{\cdot}{\varepsilon}) - \mathrm{Proj}_{\mathcal{W}_0}(W^0(\frac{\cdot}{\varepsilon}))$, $W \overset{\text{def}}{=} W^0(\frac{\cdot}{p\varepsilon})$, $f_p \overset{\text{def}}{=} W^0(\frac{\cdot}{\varepsilon})_{|\partial\Lambda}$ and $f \overset{\text{def}}{=} W_{|\partial\widetilde{\Lambda}} = W^0(\frac{\cdot}{p\varepsilon})_{|\partial\widetilde{\Lambda}}$. Observe that $W_p$ is the unique solution of the following variational formulation:

$$\begin{cases} \text{find } W_p \in \mathrm{H}^1(\Lambda) \text{ with } W_p = f_p \text{ on } \partial\Lambda \text{ such that for all } z \in \mathcal{W}_0, \\ \displaystyle\int_\Lambda \alpha\nabla W_p \cdot \nabla z \,\mathrm{d}x = 0. \end{cases}$$

Hence, we can apply (3.18) to $\eta = W_p$ and $\zeta = \mathcal{L}_p f_p$, we find

$$\|W_p - \mathcal{L}_p f_p\|_{\alpha,\Lambda} \leq C_{\alpha_f,\alpha_m} \|\mathcal{L}_p f_p\|_{\alpha_f,\Omega_f} \leq C_{\alpha_f,\alpha_m} \|\mathcal{L}_p f_p\|_{\alpha,\Lambda}.$$

It follows that

$$\|W_p\|_{\alpha,\Lambda} \leq (1 + C_{\alpha_f,\alpha_m}) \max(\alpha_f,\alpha_m) \|\nabla(\mathcal{L}_p f_p)\|_{\mathrm{L}^2(\Lambda)} \leq (1 + C_{\alpha_f,\alpha_m}) \max(\alpha_f,\alpha_m) \|\nabla(\mathcal{L}f)\|_{\mathrm{L}^2(\widetilde{\Lambda})},$$

by (4.14). Finally, by using (4.13), we find

$$\|W_p\|_{\alpha,\Lambda} \leq C \max(\alpha_f,\alpha_m) \|f\|_{\mathrm{H}^{1/2}(\partial\widetilde{\Lambda})} \leq C \max(\alpha_f,\alpha_m) p\varepsilon.$$ ∎

We can now establish the following estimate between the corrector $w^0$ given by the patch method and $W^0(\frac{\cdot}{\varepsilon})$ the corrector of the asymptotic analysis.

**Lemma 4.3.** *Let $w^0$ be the solution to Problem (3.2) for $n = 0$. Then, we have*

$$\left\|w^0 - \varepsilon W^0\left(\frac{\cdot}{\varepsilon}\right)\right\|_{\alpha,\Lambda} \leq Cp\varepsilon^2. \tag{4.16}$$

**Proof.** Note that the triangle inequality leads to

$$\left\|w^0 - \varepsilon W^0\Big(\frac{\cdot}{\varepsilon}\Big)\right\|_{\alpha,\Lambda} \leq \left\|w^0 - \mathrm{Proj}_{\mathcal{W}_0}\Big(\varepsilon W^0\Big(\frac{\cdot}{\varepsilon}\Big)\Big)\right\|_{\alpha,\Lambda} + \varepsilon\left\|\mathrm{Proj}_{\mathcal{W}_0}\Big(W^0\Big(\frac{\cdot}{\varepsilon}\Big)\Big) - W^0\Big(\frac{\cdot}{\varepsilon}\Big)\right\|_{\alpha,\Lambda}. \quad (4.17)$$

Since $w^0 = \mathrm{Proj}_{\mathcal{W}_0}(u - u^0)$, it comes that

$$\left\|w^0 - \mathrm{Proj}_{\mathcal{W}_0}\Big(\varepsilon W^0\Big(\frac{\cdot}{\varepsilon}\Big)\Big)\right\|_{\alpha,\Lambda} \leq \left\|\mathrm{Proj}_{\mathcal{W}_0}\Big(u - u^0 - \varepsilon W^0\Big(\frac{\cdot}{\varepsilon}\Big)\Big)\right\|_{\alpha,\Lambda} \leq \left\|u - u^0 - \varepsilon W^0\Big(\frac{\cdot}{\varepsilon}\Big)\right\|_{\alpha,\Lambda}. \quad (4.18)$$

According to inequality (4.17), Lemmas 4.1 and 4.2, (4.16) follows. ∎

On the one hand, we observe that

$$\|u - (u^0 + w^0)\|_{\alpha,\Lambda} \leq \|u - u^0 - \varepsilon W^0\Big(\frac{\cdot}{\varepsilon}\Big)\|_{\alpha,\Omega} + \left\|w^0 - \varepsilon W^0\Big(\frac{\cdot}{\varepsilon}\Big)\right\|_{\alpha,\Lambda} \leq C\varepsilon^2 + Cp\varepsilon^2 \leq Cp\varepsilon^2.$$

On the other hand, this implies

$$\begin{aligned}\|u - (u^0 + w^0)\|_{\alpha,\Omega} &\leq \left\|u - u^0 - \varepsilon W^0\Big(\frac{\cdot}{\varepsilon}\Big)\right\|_{\alpha,\Omega} + \left\|w^0 - \varepsilon W^0\Big(\frac{\cdot}{\varepsilon}\Big)\right\|_{\alpha,\Omega}\\ &\leq \left\|u - u^0 - \varepsilon W^0\Big(\frac{\cdot}{\varepsilon}\Big)\right\|_{\alpha,\Omega} + \left\|w^0 - \varepsilon W^0\Big(\frac{\cdot}{\varepsilon}\Big)\right\|_{\alpha,\Lambda} + \varepsilon\left\|W^0\Big(\frac{\cdot}{\varepsilon}\Big)\right\|_{\alpha_m,\Omega\setminus\Lambda}\\ &\leq C\varepsilon^2 + Cp\varepsilon^2 + \varepsilon\left\|W^0\Big(\frac{\cdot}{\varepsilon}\Big)\right\|_{\alpha_m,\Omega\setminus\Lambda}.\end{aligned}$$

By using (4.12) for $\varrho_1$, which is the largest radius of the circle included in $\Lambda$, for $\varepsilon < \frac{\varrho_1}{R_0}$, we find

$$\left\|W^0\Big(\frac{\cdot}{\varepsilon}\Big)\right\|_{\alpha_m,\Omega\setminus\Lambda} \leq C\frac{\varepsilon}{\varrho_1} \leq Cp\varepsilon,$$

which implies that

$$\left\|u - (u^0 + w^0)\right\|_{\alpha,\Omega} \leq Cp\varepsilon^2. \quad (4.19)$$

We give now an estimate for $\|\frac{\partial w^0}{\partial n}\|_{\mathcal{X}'}$.

**Lemma 4.4.** *There exists a constant $C > 0$, independent of $\varepsilon$ and $p$, such that*

$$\left\|\frac{\partial w^0}{\partial n}\right\|_{\mathcal{X}'} \leq Cp^{3/2}\varepsilon^2 \leq \frac{C\varepsilon^2}{\mathrm{diam}(\Lambda)^{3/2}}. \quad (4.20)$$

**Proof.** We evaluate first $\|f\|_{\mathrm{H}^{1/2}(\partial\widetilde{\Lambda})}$ with respect to $\|f_p\|_{\mathcal{X}}$. To this aim, we define the linear operator $\mathcal{D}_p$ as follows

$$\begin{array}{rccc}\mathcal{D}_p: & \mathscr{H}(\partial\Lambda) & \longrightarrow & \mathscr{H}(\partial\widetilde{\Lambda})\\ & f_p & \longmapsto & f\end{array} \quad (4.21)$$

where $\mathscr{H}$ could be $\mathrm{L}^2$, or $\mathrm{H}^{1/2}$ or $\mathrm{H}^1$. On the one hand, we observe that

$$\|f\|^2_{\mathrm{L}^2(\partial\widetilde{\Lambda})} = \int_{\partial\widetilde{\Lambda}} |f(u)|^2 \,\mathrm{d}S = \int_{\partial\widetilde{\Lambda}} |f_p(u/p)|^2 \,\mathrm{d}S = p\,\|f_p\|^2_{\mathrm{L}^2(\partial\Lambda)},$$

and

$$\|\nabla f\|^2_{\mathrm{L}^2(\partial\widetilde{\Lambda})} = \int_{\partial\widetilde{\Lambda}} \frac{1}{p^2}\,|\nabla f_p(u/p)|^2 \,\mathrm{d}S = \frac{1}{p}\,\|\nabla f_p\|^2_{\mathrm{L}^2(\partial\Lambda)}$$

for all $p \geq 1$. We deduce that

$$\|\mathcal{D}_p\|_{\mathrm{L}^2} = \sup_{f_p\in\mathrm{L}^2(\partial\Lambda)} \frac{\|f\|_{\mathrm{L}^2(\partial\widetilde{\Lambda})}}{\|f_p\|_{\mathrm{L}^2(\partial\Lambda)}} = \sqrt{p},$$

$$\|\mathcal{D}_p\|_{\mathrm{H}^1} = \sup_{f_p\in\mathrm{H}^1(\partial\Lambda)} \frac{\|f\|_{\mathrm{H}^1(\partial\widetilde{\Lambda})}}{\|f_p\|_{\mathrm{H}^1(\partial\Lambda)}} \leq \sqrt{p} + \frac{1}{\sqrt{p}} \text{ with } p \geq 1.$$

By interpolating [8], we find

$$\|\mathcal{D}_p\|_{\mathrm{H}^{1/2}} \leq C \|\mathcal{D}_p\|_{\mathrm{L}^2}^{1/2} \|\mathcal{D}_p\|_{\mathrm{H}^1}^{1/2} \leq C\sqrt{1+p},$$

with a constant $C > 0$ independent of $\varepsilon > 0$ and $p \geq 1$. Let $\theta \in \mathrm{C}^\infty(\widetilde{\Lambda}, [0,1])$ be a cut-off function such that $\theta(x) = 1$ for $x$ in a small tubular neighborhood $T$ of $\partial\widetilde{\Lambda}$ and $\theta(x) = 0$ outside a small tubular neighborhood containing $T$ and $\theta_p = \theta \circ (h_p)^{-1}$. Using the regularity of $w^0$ and Green's formula, it comes that

$$\int_\Lambda \alpha \nabla w^0 \cdot \nabla(\theta_p \mathcal{L}_p f_p)\,\mathrm{d}x = \Big\langle \frac{\partial w^0}{\partial n}, f_p \Big\rangle_{\mathcal{X}',\mathcal{X}}$$

for all $f_p \in \mathrm{H}^{1/2}(\partial\Lambda)$. Denoting $\widetilde{\mathcal{T}} = \{x \in \widetilde{\Lambda} : \theta(x) > 0\}$ and $\mathcal{T} = \frac{\widetilde{\mathcal{T}}}{p}$, we deduce that

$$\Big|\Big\langle \frac{\partial w^0}{\partial n}, f_p \Big\rangle_{\mathcal{X}',\mathcal{X}}\Big| \leq \alpha_m \Big\|\nabla w^0\Big\|_{\mathrm{L}^2(\mathcal{T})} \|\nabla(\theta_p \mathcal{L}_p f_p)\|_{\mathrm{L}^2(\Lambda)} = \alpha_m \Big\|\nabla w^0\Big\|_{\mathrm{L}^2(\mathcal{T})} \|\nabla(\theta\mathcal{L}f)\|_{\mathrm{L}^2(\widetilde{\Lambda})}.$$

However, we have

$$\begin{aligned}\|\nabla(\theta\mathcal{L}f)\|_{\mathrm{L}^2(\widetilde{\Lambda})} &\leq \|\theta\|_{\mathrm{W}^{1,\infty}(\widetilde{\Lambda})} \|\mathcal{L}f\|_{\mathrm{H}^1(\widetilde{\Lambda})} \leq C \|f\|_{\mathrm{H}^{1/2}(\partial\widetilde{\Lambda})} \\ &\leq C \|\mathcal{D}_p f_p\|_{\mathrm{H}^{1/2}(\partial\widetilde{\Lambda})} \leq C \|\mathcal{D}_p\|_{\mathrm{H}^{1/2}} \ \|f_p\|_{\mathcal{X}} \leq C\sqrt{1+p}\,\|f_p\|_{\mathcal{X}},\end{aligned}$$

and

$$\Big\|\nabla w^0\Big\|_{\mathrm{L}^2(\mathcal{T})} \leq \Big\|\nabla w^0 - \varepsilon \nabla W^0\Big(\frac{\cdot}{\varepsilon}\Big)\Big\|_{\mathrm{L}^2(\Lambda)} + \varepsilon \Big\|\nabla W^0\Big(\frac{\cdot}{\varepsilon}\Big)\Big\|_{\mathrm{L}^2(\mathcal{T})}. \tag{4.22}$$

On the one hand, Lemma 4.3 leads to

$$\Big\|\nabla w^0 - \varepsilon \nabla W^0\Big(\frac{\cdot}{\varepsilon}\Big)\Big\|_{\mathrm{L}^2(\Lambda)} \leq Cp\varepsilon^2.$$

On the other hand, (4.12) and since $|x| > \varrho_1$ for $x \in \widetilde{\mathcal{T}}$, we get

$$\Big\|\nabla W^0\Big(\frac{\cdot}{\varepsilon}\Big)\Big\|_{\mathrm{L}^2(\mathcal{T})} = \Big\|\nabla W^0\Big(\frac{\cdot}{p\varepsilon}\Big)\Big\|_{\mathrm{L}^2(\widetilde{\mathcal{T}})} \leq Cp\varepsilon.$$

Consequently, we obtain

$$\Big|\Big\langle \frac{\partial w^0}{\partial n}, f_p \Big\rangle_{\mathcal{X}',\mathcal{X}}\Big| \leq Cp\varepsilon^2 \sqrt{1+p}\,\|f_p\|_{\mathcal{X}} \leq C\varepsilon^2 p^{3/2}\,\|f_p\|_{\mathcal{X}},$$

which proves the lemma. ∎

## 5. Numerical study

### 5.1. Numerical multi-scale patch method

In this section, we present a multi-scale discrete patch method defined by the iterative patch procedure (3.1) and (3.2). To this aim, we introduce $\mathcal{T}^\Lambda$ and $\mathcal{T}^\Omega$ two non-degenerated non-overlapping triangulations, the respective polygonal domain partitions of $\Lambda$ and $\Omega$. More precisely, $\mathcal{T}^\Lambda$ is a refined mesh of $\Lambda$ with a maximal size equal to $h$ that accounts for the inclusion and $\mathcal{T}^\Omega$ is a relatively coarse mesh of $\Omega$ with a maximal size $H$ that is generally not conformal to the inclusion. However, for the sake of simplicity, $\mathcal{T}^\Omega$ is taken conformal to the boundary of $\Lambda$. In order to approximate $u^n$ and $w^n$, we first introduce the following Lagrange finite element spaces, for $k$ a chosen degree:

$$\begin{aligned}\mathcal{V}_0^H &\stackrel{\text{def}}{=} \{v \in \mathrm{C}^0(\overline{\Omega}) : \text{ for all } K \text{ triangle of } \mathcal{T}^\Omega,\ v_{|K} \in P^k(K),\ v_{|\Gamma_\mathrm{D}} = 0\} \subset \mathcal{V}_0,\\ \mathcal{W}_0^h &\stackrel{\text{def}}{=} \{v \in \mathrm{C}^0(\overline{\Omega}) : \text{ for all } K \text{ triangle of } \mathcal{T}^\Lambda,\ v_{|K} \in P^k(K),\ v_{|\Omega\setminus\Lambda} = 0\} \subset \mathcal{W}_0.\end{aligned}$$

We still use the convention $w_h^{-1} = u_H^{-1} = 0$ for the simplicity of the definition of the iterations. Hence for any $w_h^{n-1}$ and $u_H^{n-1}$ given, $n \geq 0$, we first solve the following macro problem on $\mathcal{T}^\Omega$:

$$\begin{cases} \text{find } u_H^n \in \mathcal{V}_0^H \text{ such that for all } v_H \in \mathcal{V}_0^H, \\ \displaystyle\int_\Omega \alpha_m \nabla u_H^n \cdot \nabla v_H \,\mathrm{d}x = \int_\Omega f v_H \,\mathrm{d}x + \int_{\Gamma_\mathrm{N}} h v_H \,\mathrm{dS} \\ \displaystyle -\int_{\Omega_f} (\alpha_f - \alpha_m) \nabla u_H^{n-1} \cdot \nabla v_H \,\mathrm{d}x - \int_\Lambda \alpha \nabla w_h^{n-1} \cdot \nabla v_H \,\mathrm{d}x, \end{cases} \tag{5.1}$$

and then we solve the following micro problem on $\mathcal{T}^\Lambda$:

$$\begin{cases} \text{find } w_h^n \in \mathcal{W}_0^h \text{ such that for all } v_h \in \mathcal{W}_0^h, \\ \displaystyle\int_\Lambda \alpha \nabla w_h^n \cdot \nabla v_h \,\mathrm{d}x = \int_\Lambda f v_h \,\mathrm{d}x - \int_\Lambda \alpha \nabla u_H^n \cdot \nabla v_h \,\mathrm{d}x. \end{cases} \tag{5.2}$$

From a numerical viewpoint, the micro and macro coupling terms in (5.1) and (5.2) are computed using standard (but eventually composite) Gauss-quadrature formulas on the macro and micro meshes, respectively. Clearly, the solution $w_h^{n-1}$ to the micro problem (5.2) (resp. $u_H^n$ to the macro problem (5.1)) is implicitly employed in the macro problem (5.1) (resp. the micro problem (5.2)) through its orthogonal projection onto the space $\mathcal{V}_0^H$ (resp. $\mathcal{W}_0^h$) with respect to the scalar product $\langle \cdot, \cdot \rangle_{\alpha,\Lambda}$ (more rigorously by the scalar product induced by approximate integration). Let

$$u_{hH}^n \stackrel{\text{def}}{=} u_H^n + w_h^n. \tag{5.3}$$

The reader may notice that $u_{hH}^n$ is an approximate solution of $u$ (see (2.4)) on the $\mathrm{n}^{\mathrm{th}}$ iteration. We denote by $\mathcal{T}^{\mathrm{ref}}$ a regular mesh with a maximal size $h_{\mathrm{ref}}$ conformal to both boundaries $\partial\Lambda$ and $\Gamma^\varepsilon$. The reference solution $u_{\mathrm{ref}}$, used later in the numerical simulations, is the solution to the discrete variational formulation:

$$\begin{cases} \text{find } u \in \mathcal{V}_0^{h_{\mathrm{ref}}} \text{ such that for all } v \in \mathcal{V}_0^{h_{\mathrm{ref}}}, \\ \displaystyle\int_{\Omega_m} \alpha_m \nabla u \cdot \nabla v \,\mathrm{d}x + \int_{\Omega_f} \alpha_f \nabla u \cdot \nabla v \,\mathrm{d}x = \int_\Omega f v \,\mathrm{d}x + \int_{\Gamma_\mathrm{N}} h v \,\mathrm{dS}. \end{cases} \tag{5.4}$$

Assume that $w_h^n$ and $u_H^n$ converge to $w_h$ and $u_H$, respectively, as $n$ tends to $\infty$. It follows by adding (5.1) and (5.2) that

$$\int_\Omega \alpha \nabla (u_H + w_h) \cdot \nabla (v_H + v_h) \,\mathrm{d}x = \int_\Omega f (v_H + v_h) \,\mathrm{d}x + \int_{\Gamma_N} h (v_H + v_h) \,\mathrm{d}S,$$

for all $v_H \in \mathcal{V}_0^H$ and all $v_h \in \mathcal{W}_0^h$ which means that $u_{hH} = u_H + w_h$ is the best approximation to the solution on the sum of the approximation spaces $\mathcal{V}_0^H + \mathcal{W}_0^h$.

### 5.2. **Test problem definition**

The numerical tests presented below are performed on a simple square geometry $\Omega = (-L, L) \times (-L, L)$ with $L = 10$. We assume that the boundary $\Gamma$ is split into two distinct parts, namely, Dirichlet and Neumann boundaries denoted by $\Gamma_\mathrm{D} = (-L, L) \times \{-L\} \cup (-L, L) \times \{L\}$ and $\Gamma_\mathrm{N} = \{-L\} \times (-L, L) \cup \{L\} \times (-L, L)$, respectively, where homogeneous conditions are prescribed. Furthermore, we suppose that the inclusion is a disk of center $(3, 2)$ and radius $\varepsilon$ (see Figure 5.1), while the patch domain is a square $\Lambda = (3 - l, 3 + l) \times (2 - l, 2 + l)$. Unless otherwise stated, the values of $\varepsilon$ and $l$ are 1 and 4, respectively. We choose the volumetric source term $f$ equal to $10 \cos(\frac{\pi}{4L} x) \cosh(\frac{y}{2L})$. Note that the reference solution (see Figure 5.2a) is computed on the reference mesh $\mathcal{T}^{\mathrm{ref}}$ (see Figure 5.2b) while all the numerical simulations are performed using a macro mesh $\mathcal{T}^\Omega$ conformal to the patch boundary $\partial\Lambda$. We use quadratic finite elements ($\mathrm{k} = 2$) and standard fourth-order Gauss-quadrature formulas

on the triangles of both meshes. However, for the coupling terms, we utilize composite quadrature formulas, dividing each triangle into three ones, for a higher accuracy integration.

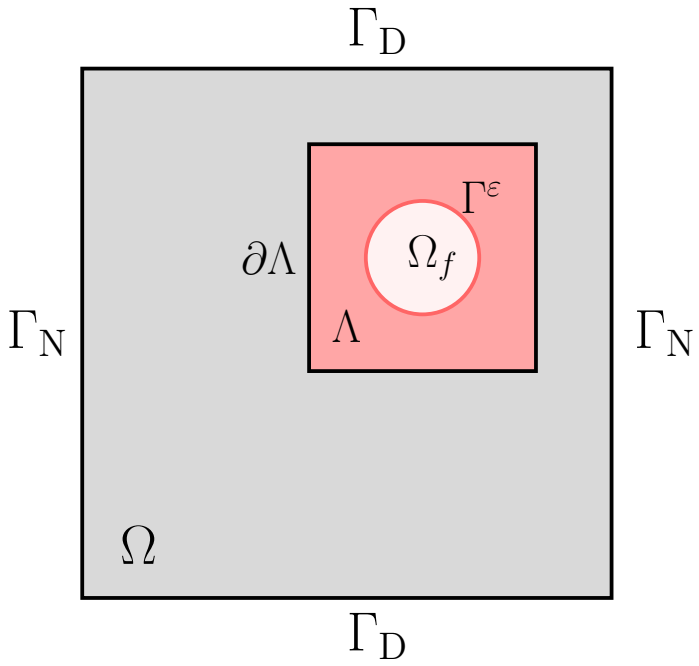


Figure 5.1. A simple square domain containing an inclusion and a patch.

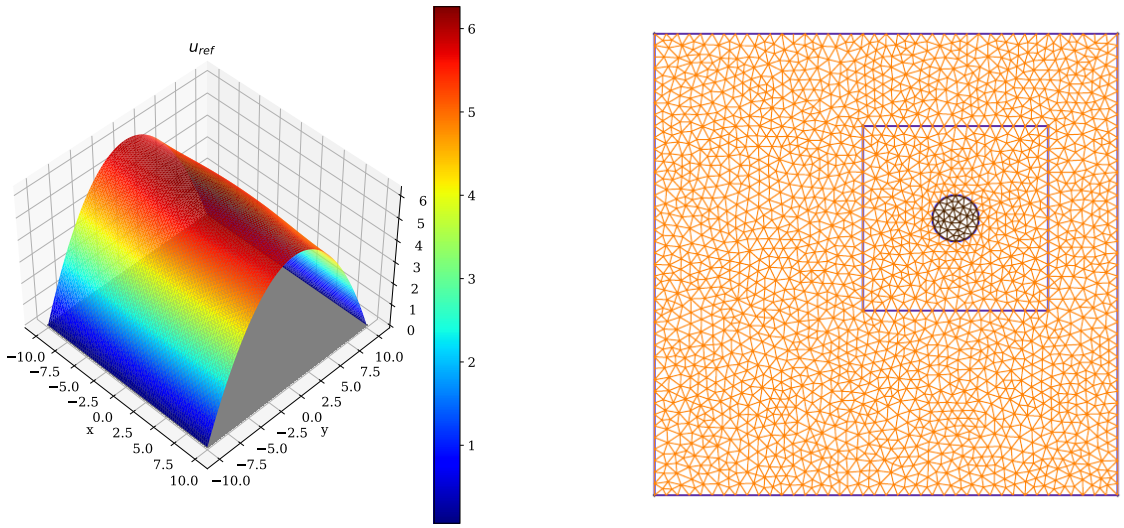


(a) Reference solution ($\alpha_m = 75$ and $\alpha_f = 100$)

(b) Conformal mesh

Figure 5.2. A reference solution and an example of a conformal mesh with $h_{\text{ref}} = \frac{L}{20}$

## 5.3. **Numerical convergence of the iterations**

### 5.3.1. *Convergence of the iterations with a single mesh for the reference, micro and macro models*

In this section, our goal is to test the convergence of the iterations without the influence of the difference between the meshes (and the corresponding projections) of macro and micro problems by using the same mesh for the three problems, although this situation is not really of practical interest. When the convergence occurs and since $\mathcal{V}_0^H + \mathcal{W}_0^h = \mathcal{V}_0^H = \mathcal{V}_0^{h_{\text{ref}}}$, the iterations should converge toward the reference solution up to machine precision

We consider, in the numerical simulations, several values of $\alpha_m$ and $\alpha_f$ and for $h = H = h_{\text{ref}} = \frac{L}{40}$. We illustrate the impact of the contrast between $\alpha_m$ and $\alpha_f$ on the solution by plotting the difference between the solutions associated to the reference model $u_{\text{ref}}$ and the macro model (see Figures 5.3a and 5.3b). Recall that $u_H^0$ is the approximate solution of (2.2) without any inclusion (it is the solution to (5.1) for $n = 0$).

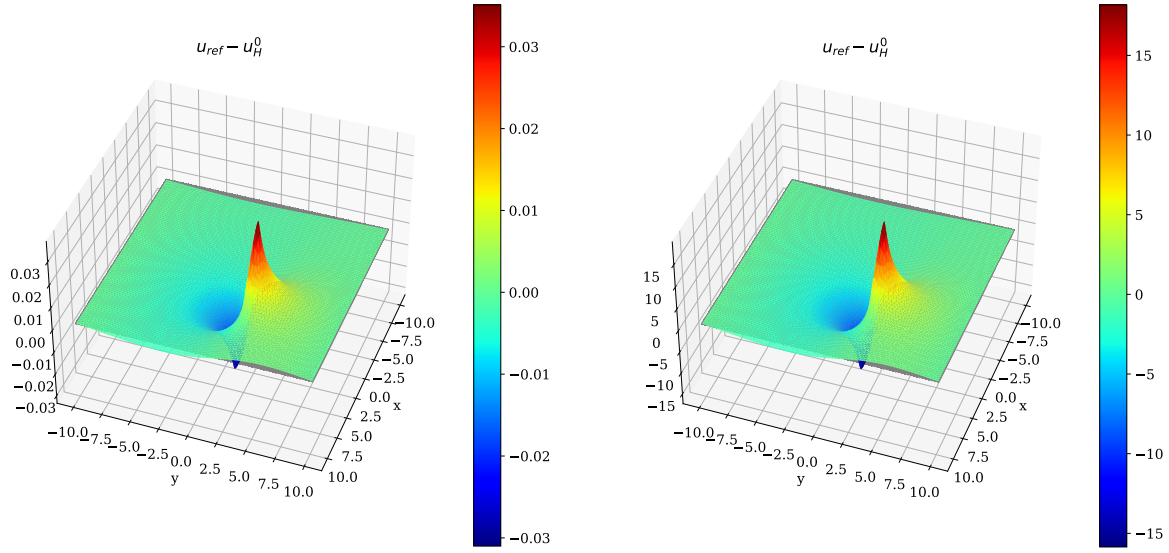


(A) $\alpha_m = 75$ and $\alpha_f = 100$ (B) $\alpha_m = 1$ and $\alpha_f = 100$

FIGURE 5.3. Plot of $u_{\text{ref}} - u_H^0$ for two different contrasts.

The relative error rate in the $\mathrm{H}^1(\Omega)$-norm between $u_{\text{ref}}$ and $u_{hH}^n$ is plotted in Figure 5.4 according to the variation of the iterations number $n$. We observe that the iterative procedure converges within few iterations. Since the convergence occurs for all tested contrast values, the results obtained by the numerical simulations are much better than expected by the theoretical results presented in Section 3.2.

### 5.3.2. *Convergence of the iterations with non-matching meshes*

In order to highlight the influence of the difference of meshes on micro and macro problems, we consider now three independent meshes. The reference solution is computed by using an adaptive mesh, where the maximum size near the inclusion is set as $h_{\text{ref}} = \frac{L}{600}$, while in the remaining domain it is $\frac{L}{80}$. Furthermore, meshes are generated for the micro and macro models, having maximal sizes $h = \frac{L}{120}$ and $H = \frac{L}{40}$, respectively. Note that the mesh for the macro model is non-conformal to the inclusion boundary $\partial\Omega_f$.

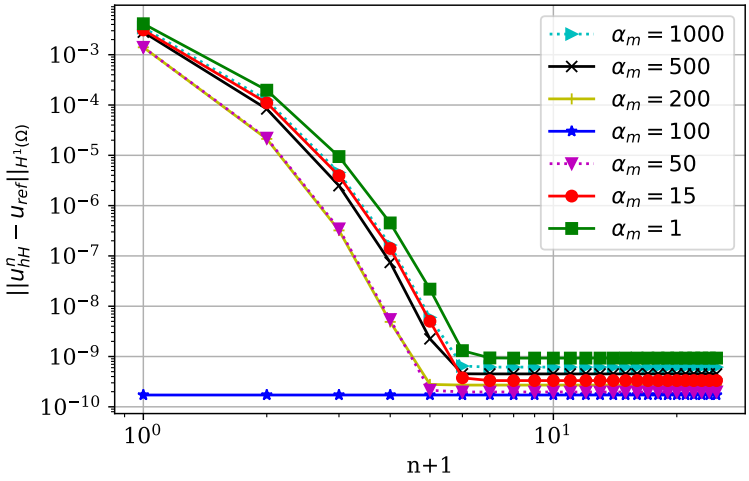


Figure 5.4. The relative error in $\mathrm{H}^1(\Omega)$-norm for different values of contrast (between $\alpha_m$ and $\alpha_f = 100$) and with the same mesh for the reference, micro and macro model ($h = H = h_{\text{ref}} = \frac{L}{40}$).

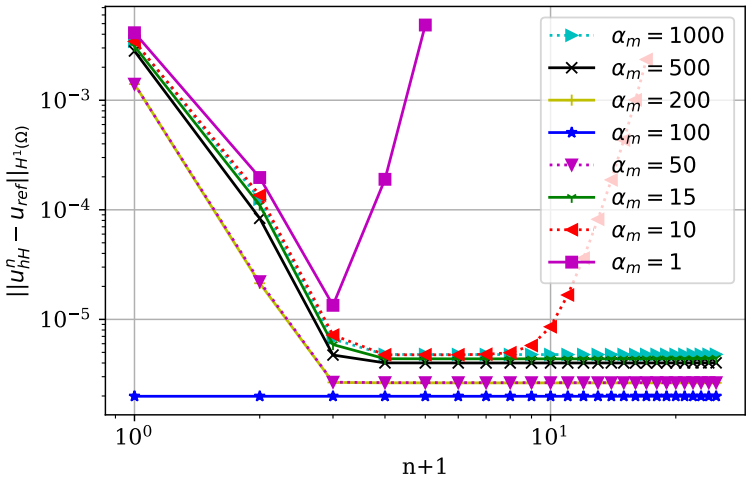


Figure 5.5. The relative error in $\mathrm{H}^1(\Omega)$-norm with respect to the variation of the number of iteration $n$ for different values of contrast between $\alpha_m$ and $\alpha_f = 100$, non-matching meshes ($h = \frac{L}{120}, H = \frac{L}{40}$) and a non-conformal macro mesh with the inclusion $\partial\Omega_f$.

We observe that if $\alpha_m \geq 15$, the iterative procedure converges quickly for the $\mathrm{H}^1(\Omega)$-norm (see Figure 5.5) but with higher relative error than in the case where the same mesh is used for the three models. While in the case where $\alpha_m < 15$, the error decreases during the first iterations, but the procedure finally diverges. Consequently, this scenario is less advantageous than the one involving

identical meshes and aligns more closely with the theoretical outcomes presented in Section 3.2 which predicts convergence for not too high contrast or for a sufficiently small inclusion. However, in both cases, the error resulting from halting after the second iteration is quite low.

Finally, we might note that the iterations convergence in the case where $\alpha_m < 15$ can be recovered by a refinement of the patch mesh (see Figure 5.6), i.e. by taking the micro mesh size $h$ sufficiently small. Here we choose $H = \frac{L}{40}$, $\alpha_m = 1$ and $\alpha_f = 100$.

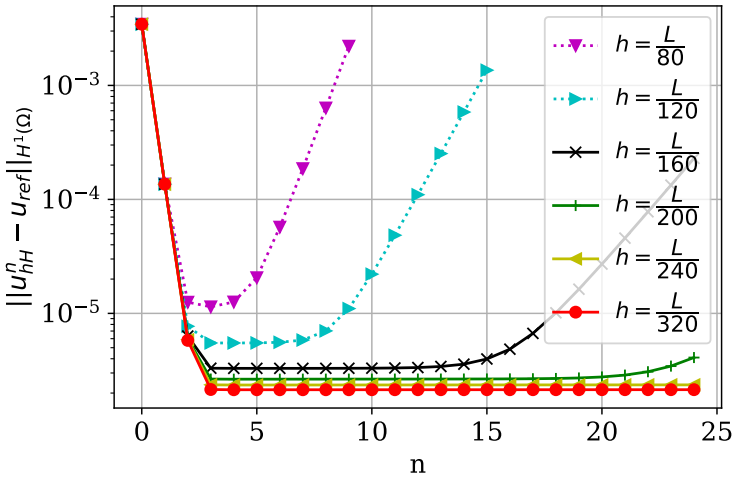


FIGURE 5.6. The relative error in $\mathrm{H}^1(\Omega)$-norm with respect to the variation of the number of iteration $n$ for different values of micro-mesh size (with $\alpha_m = 10$ and $\alpha_f = 100$), non-matching meshes ($H = \frac{L}{40}$) and a non-conformal macro mesh with the inclusion $\partial\Omega_f$.

### 5.4. **A relaxation method to recover the convergence**

As an alternative approach to the refinement of the patch mesh, we propose below a relaxation method in the case of a high contrast. Since Problem (5.2) corresponds to a descent method on the potential energy associated to the system in the direction $w_h^n$, it does not alter the iteration convergence. The non-convergence for high contrast values arises from the term $u_H^{n-1}$ in (5.1). This term follows the asymptotic expansion and ensures that $u_H^0$ is the solution without the inclusion. Furthermore, $w_h^0$ is close to the first corrector of the asymptotic expansion and globally $u_H^n$ is a smooth solution which does not take into account the local variations across the interface between the matrix and the inclusion which is handled by $w_h^n$. To decrease the influence of this term on the convergence, we propose to introduce a relaxation keeping $u_H^0$ and $w_h^0$ unchanged and, for $\beta \in (0,1)$ a relaxation coefficient, to modify from the second iteration as follows:

- denoting now $\widetilde{u}_H^n$ a solution to (5.1) for $n \geq 1$ and taking $u_H^n = \beta\widetilde{u}_H^n + (1-\beta)u_H^{n-1}$ instead $\widetilde{u}_H^n$.
- the remaining is unchanged, in particular, $w_h^n$ is still a solution to (5.2).

Note that this relaxation method is applied only to the step (5.1) and, thus, it slightly differs from the relaxation method proposed in [18]. Looking at Figure 5.7, it is clear that with a sufficiently

low relaxation coefficient (specifically, $\beta \leq 0.05$ in this scenario), our iterative approach can recover convergence even under high-contrast conditions (with $\alpha_m = 1$ and $\alpha_f = 100$). However, the cost of this restored convergence is an elevation in the required number of iterations for achieving convergence. Numerically, it seems that there is approximately a linear dependence between the largest value of $\beta$

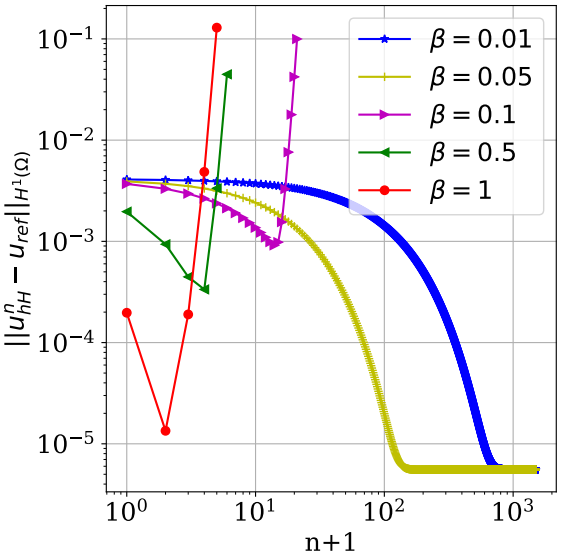


Figure 5.7. The relative error in $\mathrm{H}^1(\Omega)$-norm with respect to the variation of the number of iteration $n$ for different values of the relaxation coefficient (with $\alpha_m = 1$ and $\alpha_f = 100$), non-matching meshes ($h = \frac{L}{120}$, $H = \frac{L}{40}$) and a non-conformal macro mesh with the inclusion $\partial\Omega_f$.

ensuring the convergence and the contrast, namely $\beta = 5\,\frac{\alpha_m}{\alpha_f}$. In Figure 5.8, we found that choosing $\beta = 5\,\frac{\alpha_m}{\alpha_f}$ guarantees the convergence for a wide range of contrast and $\varepsilon$ values even though the number of iterations to reach the convergence varies.

### 5.5. **Influence of the patch size**

In this section the reference solution is computed using an adaptive mesh with a maximal size $h_{\text{ref}}$ equal to $\frac{L}{600}$ in the inclusion vicinity and $\frac{L}{80}$ in the remained domain. In order to study the effect of the patch domain size on the accuracy of the obtained solution by the multi-scale patch strategy, we plot in Figure 5.9 the relative error in $\mathrm{L}^2(\Omega)$ and $\mathrm{H}^1(\Omega)$ norms according to the patch characteristic parameter $p$ with $h = \frac{L}{80}$, $H = \frac{L}{40}$ and a non-conformal mesh with the boundary $\partial\Omega_f$ for the macro model. As expected, we observe that the relative error between $u_{hH}^0$ and $u_{\text{ref}}$, decreases in both $\mathrm{L}^2(\Omega)$ and $\mathrm{H}^1(\Omega)$ norms, when the patch size increases (see the Figure 5.9a). Note that the convergence rate of order 1 in $\mathrm{H}^1(\Omega)$-norm given by the theoretical estimate (4.19) is not fully reached for large value of $p$. This corresponds to patch sizes close to the inclusion size for which there is probably some side effects. On the other hand, the relative errors between $u_{hH}$ and $u_{\text{ref}}$, in both $\mathrm{L}^2(\Omega)$ and $\mathrm{H}^1(\Omega)$ norms, remain almost constant when the patch size varies (see the Figure 5.9b). Consequently, we conclude that the choice of a relatively small patch can be compensated by using an adequate iterations number of the proposed method.

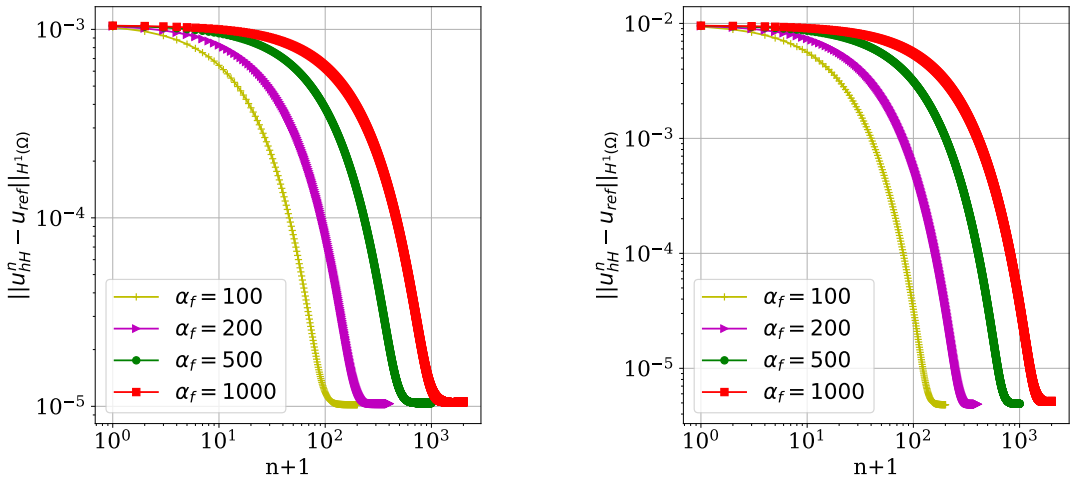


(A) $\varepsilon = 0.5$ (B) $\varepsilon = 1.5$

FIGURE 5.8. The relative error in $\mathrm{H}^1(\Omega)$-norm with respect to the variation of the number of iterations $n$ for different values of the size of the inclusion $\varepsilon$ (with $\alpha_m = 1$ and the relaxation coefficient $\beta = 5\,\dfrac{\alpha_m}{\alpha_f}$), non-matching meshes ($h = \frac{L}{120}$, $H = \frac{L}{40}$) and a non-conformal macro mesh with the inclusion $\partial\Omega_f$

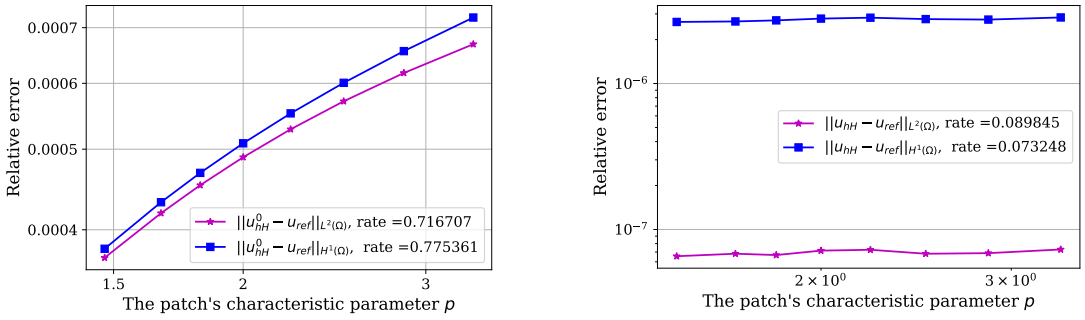


(A) First iteration (B) Last iteration

FIGURE 5.9. The relative error in $\mathrm{L}^2(\Omega)$ and $\mathrm{H}^1(\Omega)$ norms for the first ($u^0_{hH}$) and last iteration ($u_{hH}$) of the iterative method with respect to the patch characteristic parameter $p$ with $h = \frac{L}{80}$, $H = \frac{L}{40}$ and a non-conformal mesh with the macro model boundary $\partial\Omega_f$ (recall that $u^n_{hH}$ and $u_{hH}$ are defined in Section 5.1).

### 5.6. **Influence of the inclusion size**

In this section, the reference mesh (resp. the micro mesh) is conformal to disks of radii $\epsilon_1 = 1.5, \epsilon_2 = 1, \epsilon_3 = 0.5$, and $\epsilon_4 = 0.25$. The maximum size of the reference mesh (resp. the micro mesh) near each circle $i\,(1 \leq i \leq 4)$ is $h_{\text{ref}} = \epsilon_i/40$ (resp. $h = \epsilon_i/20$), while in the remaining domain, it is equal to

$L/80$ (resp. $L/40$). The macro mesh is non-conformal to the inclusion boundary $\partial\Omega_f$ and possesses a maximum size $H$ equal to $L/40$. In order to study the effect of the inclusion size on the solution accuracy, we first plot in Figure 5.10 the variation of the relative error in $\mathrm{L}^2(\Omega)$ and $\mathrm{H}^1(\Omega)$ norms according to the size of the inclusion. We observe that the relative error between $u^0_{hH}$ and $u_{\mathrm{ref}}$, in both $\mathrm{L}^2(\Omega)$ and $\mathrm{H}^1(\Omega)$ norms, decreases when the size of the inclusion decreases (see Figure 5.10a). The convergence rates are approximately of order 2 for both $\mathrm{L}^2(\Omega)$ and $\mathrm{H}^1(\Omega)$ relative error norms. Such a convergence rate confirms the result in (4.19). Furthermore, the Figure 5.10b shows that the relative error between $u_{hH}$ and $u_{\mathrm{ref}}$, in both $\mathrm{L}^2(\Omega)$ and $\mathrm{H}^1(\Omega)$ norms, also decreases and is several order of magnitude smaller than for the first iteration. However, a certain saturation of the error can be observed, probably due to the difference in element sizes between the reference mesh and the macro and micro meshes. We plot in the Figure 5.11 the relative error in $\mathrm{H}^1(\Omega)$ norm according to

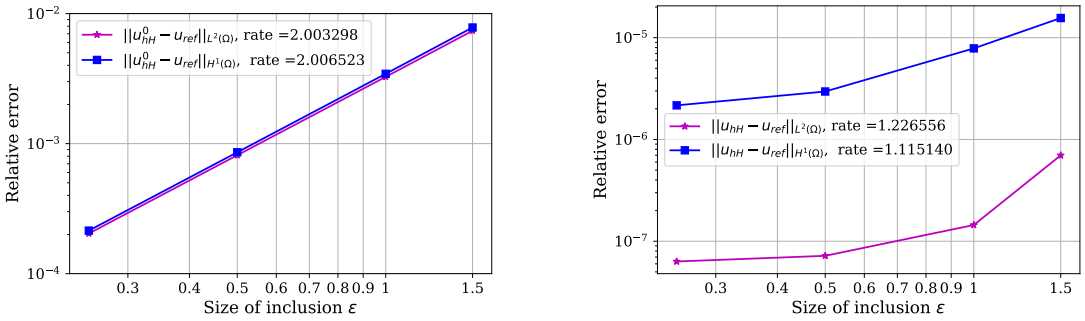


(A) First iteration

(B) Last iteration

Figure 5.10. The relative error in $\mathrm{L}^2(\Omega)$ and $\mathrm{H}^1(\Omega)$ norms according to the size of the inclusion $\varepsilon$ with a non-conformal mesh with the macro model boundary $\partial\Omega_f$.

the number of iterations $n$ for three values of $\varepsilon$ with $\alpha_m = 5$, $\alpha_f = 100$, $h_{\mathrm{ref}} = \frac{L}{2000}$, $h = \frac{\varepsilon}{20}$, $H = \frac{L}{40}$ and a non-conformal mesh with the boundary $\partial\Omega_f$ for the macro model. We observe that the iterative method diverges when $\varepsilon = 1$ but converges for smaller values of $\epsilon$, specifically $\varepsilon \leq 0.5$, confirming the outcome stated in Proposition 3.4.

## Conclusion

We presented in this work an iterative patch method for a problem with a small inhomogeneity. The main interest of this method is that it starts from the problem without inclusion, which allows to use a standard code to compute the large scale solution without meshing the inclusion. The method build a local corrector on a patch surrounding the inclusion leading to a robust solution as long as the inclusion is small enough (or the contrast between the coefficient is small enough) and the patch is sufficiently large. Furthermore, an iterative procedure allows to converge to the best finite element approximation, at least for a small inclusion or contrast as well.

We obtained some theoretical results for the iterations convergence of our patch method and we established some convergence order with respect to the inclusion and patch sizes. These results, together with the presented numerical examples, indicate that the first iteration corrector allows to improve the solution in all the cases. This means that in many cases, no supplementary iteration is necessary to get an accurate approximation.

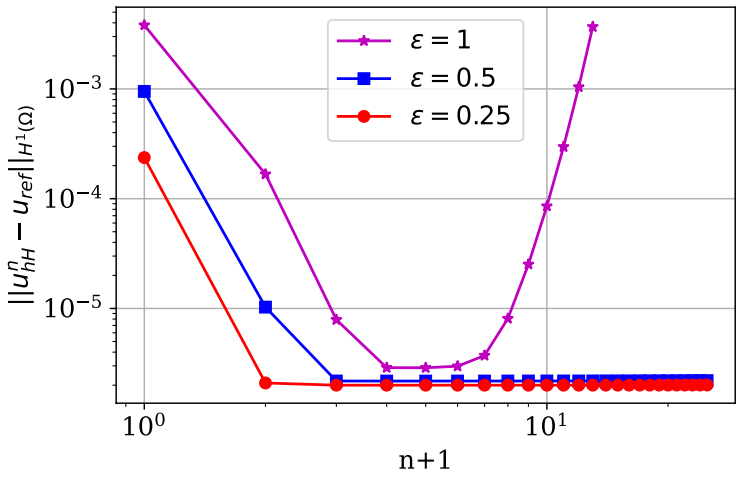


FIGURE 5.11. Evolution through iterations of the relative error in $H^1(\Omega)$-norms for three inclusion sizes.

The numerical examples highlight that the numerical multi-scale patch method convergence is not guaranteed for high values of the contrast of the stiffness in accordance with our theoretical results. For an unclear reason, this limitation is not noted in the numerical results when the meshes for the micro and macro problems are the same (which of course does not really correspond to a situation in agreement with the objectives of the proposed method), and also when the mesh for the micro problem is sufficiently refined. We proposed then a relaxation method to recover the convergence for arbitrary meshes.

Some natural perspectives for further work are extensions to the nonlinear case of finite deformation problems and to the case of multiple inclusions.

## References

[1] Habib Ammari and Hyeonbae Kang. *Reconstruction of small inhomogeneities from boundary measurements*, volume 1846 of *Lecture Notes in Mathematics*. Springer, 2004.

[2] Habib Ammari and Abdessatar Khelifi. Electromagnetic scattering by small dielectric inhomogeneities. *J. Math. Pures Appl. (9)*, 82(7):749–842, 2003.

[3] Y. A. Antipov and P. Schiavone. On the uniformity of stresses inside an inhomogeneity of arbitrary shape. *IMA J. Appl. Math.*, 68(3):299–311, 2003.

[4] Makrem Arfaoui, Mohamed Rafik Ben Hassine, Maher Moakher, Yves Renard, and Grégory Vial. Multi-scale asymptotic expansion for a small inclusion in elastic media. *J. Elasticity*, 131(2):207–237, 2018.

[5] A. Bendali and K. Lemrabet. The effect of a thin coating on the scattering of a time-harmonic wave for the Helmholtz equation. *SIAM J. Appl. Math.*, 56(6):1664–1693, 1996.

[6] A. Bendali, A. Makhlouf, and S. Tordeux. Field behavior near the edge of a microstrip antenna by the method of matched asymptotic expansions. *Q. Appl. Math.*, 69(4):691–721, 2011.

[7] Elena Beretta, Eric Bonnetier, Elisa Francini, and Anna L. Mazzucato. Small volume asymptotics for anisotropic elastic inclusions. *Inverse Probl. Imaging*, 6(1):1–23, 2012.

[8] Jöran Bergh and Jörgen Löfström. *Interpolation spaces: an introduction*, volume 223 of *Grundlehren der Mathematischen Wissenschaften*. Springer, 2012.

[9] Tahar Zamène Boulmezaoud. Inverted finite elements: a new method for solving elliptic problems in unbounded domains. *M2AN, Math. Model. Numer. Anal.*, 39(1):109–145, 2005.

[10] Anthony Chagneau. *Méthode de zoom structural étendue aux hétérogénéités non linéaires*. PhD thesis, Université Montpellier (France), 2019.

[11] Marc Dambrine and Grégory Vial. Influence of a boundary perforation on the Dirichlet energy. *Control Cybern.*, 34(1):117–136, 2005.

[12] Marc Dambrine and Grégory Vial. A multiscale correction method for local singular perturbations of the boundary. *ESAIM, Math. Model. Numer. Anal.*, 41(1):111–127, 2007.

[13] Loic Daridon, David Dureisseix, Sylvain Garcia, and Stéphane Pagano. Changement d'échelles et zoom structural. In *10e colloque national en calcul des structures*, 2011. Clé–USB.

[14] Victorita Dolean, Pierre Jolivet, and Frédéric Nataf. *An introduction to domain decomposition methods: algorithms, theory, and parallel implementation*. Society for Industrial and Applied Mathematics, 2015.

[15] J. D. Eshelby. The determination of the elastic field of an ellipsoidal inclusion, and related problems. *Proc. R. Soc. Lond., Ser. A*, 241:376–396, 1957.

[16] J. D. Eshelby. The elastic field outside an ellipsoidal inclusion. *Proc. R. Soc. Lond., Ser. A*, 252:561–569, 1959.

[17] Giuseppe Geymonat, Françoise Krasucki, and Stefano Lenci. Mathematical analysis of a bonded joint with a soft thin adhesive. *Math. Mech. Solids*, 4(2):201–225, 1999.

[18] Roland Glowinski, Jiwen He, Alexei Lozinski, Jacques Rappaz, and Joël Wagner. Finite element approximation of multi-scale elliptic problems using patches of elements. *Numer. Math.*, 101(4):663–687, 2005.

[19] Allaire Grégoire. *Shape optimization by the homogenization method*, volume 146 of *Applied Mathematical Sciences*. Springer, 2002.

[20] Derek J. Hansen, Clair Poignard, and Michael S. Vogelius. Asymptotically precise norm estimates of scattering from a small circular inhomogeneity. *Appl. Anal.*, 86(4):433–458, 2007.

[21] Mohamed Rafik Ben Hassine. *Asymptotic and numerical study of fine inclusions in elastic domains*. PhD thesis, Université de Lyon (France); École nationale d'ingénieurs de Tunis (Tunisie), 2017.

[22] Arnaud Heibig, Nidhal Mannai, Adrien Petrov, and Yves Renard. A thick-point approximation of a small body embedded in an elastic medium: justification with an asymptotic analysis. *Z. Angew. Math. Mech.*, 101(10): article no. e202000170 (19 pages), 2021.

[23] E. Kröner. Modified Green functions in the theory of heterogeneous and/or anisotropic linearly elastic media. In *Micromechanics and Inhomogeneity: The Toshio Mura 65th Anniversary Volume*, pages 197–211. Springer, 1990.

[24] E. Kröner, J. Gittus, and J. Zarka. *Modelling Small Deformations of Polycrystals*. Elsevier Applied Science Publisher, 1986.

[25] Shaofan Li, Roger Sauer, and Gang Wang. A circular inclusion in a finite domain I. The Dirichlet-Eshelby problem. *Acta Mech.*, 179(1):67–90, 2005.

[26] Eric Lignon. *Modélisation multi-échelles de nappes fibrées en compression*. PhD thesis, École Polytechnique X (France), 2011.

[27] J.-L. Lions and E. Magenes. *Problèmes aux limites non homogènes et applications. Vol. 1*, volume 17 of *Travaux et recherches mathématiques*. Dunod, 1968.

[28] Alexei Lozinski, Jacques Rappaz, and Joël Wagner. Finite element method with patches for Poisson problems in polygonal domains. *ESAIM, Proc.*, 21:45–64, 2007. Journées d'Analyse Fonctionnelle et Numérique en l'honneur de Michel Crouzeix.

[29] P Mazilu. On the theory of linear elasticity in statistically homogeneous media. *Rev. Roum. Math. Pures Appl.*, 17(2):261–273, 1972.

[30] Vittoria Rezzonico, Alexei Lozinski, Marco Picasso, Jacques Rappaz, and Joël Wagner. Multiscale algorithm with patches of finite elements. *Math. Comput. Simul.*, 76(1-3):181–187, 2007.

[31] Enrique Sánchez-Palencia. Problèmes de perturbations liés aux phénomènes de conduction à travers des couches minces de grande résistivité. *J. Math. Pures Appl. (9)*, 53:251–269, 1974.

[32] P. Schiavone. Neutrality of the elliptic inhomogeneity in the case of non-uniform loading. *Int. J. Eng. Sci.*, 41(18):2081–2090, 2003.

[33] Grégory Vial. *Analyse multi-échelle et conditions aux limites approchées pour un probleme avec couche mince dans un domainea coin*. PhD thesis, École Normale Supérieure de Cachan, Paris, 2003.